Finite-sample performance analysis of widely-linear multiuser receivers for DS-CDMA systems

Angela Sara Cacciapuoti, Giacinto Gelli, Luigi Paura, and Francesco Verde

***Abstract*—This paper tackles the theoretical performance analysis of widely-linear (WL) multiuser receivers for direct-sequence code-division multiple-access (DS-CDMA) systems, as well as their comparison with conventional linear (L) ones. In particular, receivers based on the minimum output-energy (MOE) criterion are considered, since they offer a good tradeoff between performance and complexity and, moreover, lend to some simplifications in the analysis. After comparing the ideal signal-to-interference-plus-noise-ratio (SINR) performances of the WL-MOE and L-MOE receivers, the paper establishes finite-sample performance results for two typical data-estimated implementations. Specifically, by adopting a first-order perturbative approach, the SINR degradation of the data-estimated WL-MOE receivers is accurately evaluated and compared with that of its linear counterpart. Simulation results are provided to validate and complement the theoretical analysis.**

***Index Terms*—Performance analysis, proper and improper random processes, multiuser detection, direct-sequence code-division multiple-access (DS-CDMA) systems, linear and widely-linear receiving techniques.**

I. INTRODUCTION

DUring the last two decades, starting from the seminal work of Verdú [1], a great bulk of research activities has been devoted to multiuser detection (MUD), as an effective means to combat the multiple-access interference (MAI), which is the predominant source of performance degradation in (nonorthogonal) direct-sequence (DS) code-division multiple-access (CDMA) systems. Among MUD techniques, *linear* MUD (L-MUD) ones, such as the decorrelating receiver [2], the minimum mean-square-error (MMSE) [3] one, and the minimum output-energy (MOE) [4] one, have been investigated in depth, since they offer convenient tradeoffs between performance, complexity, robustness, amount of *a priori* information, and ease of adaptive implementation.

Most L-MUD techniques assume that the complex envelope $r(t)$ of the received signal is modeled as a *proper* [5] random process, exploiting hence only the information contained in its statistical autocorrelation function $R_{rr}(t,\tau) \stackrel{\triangle}{=} \mathrm{E}[r(t)\, r^*(t-\tau)]$. When, however, the DS-CDMA signal and/or the disturbance are *improper* [5], well-established results in detection and estimation theory [6] state that linear receivers can be outperformed by *widely-linear* (WL) ones, which jointly elaborate the received signal $r(t)$ and its complex conjugate $r^*(t)$, in order to exploit also the information contained in their statistical *cross-correlation* function $R_{rr^*}(t,\tau) \stackrel{\triangle}{=} \mathrm{E}[r(t)\, r(t-\tau)]$. Many digitally modulated signals of practical interest are improper, such as ASK, differential BPSK (DBPSK), offset QPSK (OQPSK), offset QAM (OQAM), MSK and its variant Gaussian MSK (GMSK). Motivated from previous observations, in recent years several papers [7], [8], [9], [10] proposed different WL-MUD techniques for DS-CDMA systems with improper signals and/or disturbances, by extending concepts from the classical L-MUD theory. In particular, WL versions of the major L-MUD receivers have been proposed and studied, such as the WL decorrelating receiver [9], [11], the WL-MMSE one [7], [8], [12], the WL-MOE one [10], [11], and the min/max WL-MOE one [13].

In all the above-mentioned papers, the performance advantage of the WL-MUD receivers over their linear counterparts has been assessed mainly by means of computer simulations. Recently, with reference to DS-CDMA systems employing BPSK modulation, a few contributions addressing the theoretical performance analysis of WL-MUD techniques appeared in the literature. In [12], the asymptotic (in the number of users) performance analysis of the WL decorrelating and WL-MMSE receivers was carried out, by extending to the WL framework classical analysis tools already developed by Tse and Hanly [15] for L-MUD techniques (a similar study was proposed in [14]). A non-asymptotic performance analysis was instead considered in [16], which provides an algebraic proof that WL-MUD receivers outperform L-MUD ones, and explicitly assesses the expected performance gain in the two-users case. The common conclusion of these studies (see also [17]) is that the performance advantage of WL-MUD receivers over L-MUD ones is twofold: *the input SNR is doubled and the number of effective interferers is halved.* As a consequence, for a fixed processing gain N, the number of users that can be accommodated by a DS-CDMA system employing WL-MUD is doubled [12], [14], [16] compared to L-MUD. In other words, unlike L-MUD, WL-MUD can be successfully employed not only when the number of users J is smaller than or equal to N (*underloaded system*), but also when $N < J \leq 2\,N$ (*overloaded system*). However, none of the aforementioned papers on WL-MUD carried out a detailed study of the conditions on the channels and codes that assure perfect MAI suppression in the absence of noise. Thus, a

Manuscript received ....; revised .....and..... This work is partially supported by Italian National project Wireless 8O2.16 Multi-antenna mEsh Networks (WOMEN) under grant number 2005093248. The associate editor coordinating the review of this manuscript and approving it for publication was Dr. Eran Fishler.

The authors are with Dipartimento di Ingegneria Elettronica e delle Telecomunicazioni, Università degli Studi di Napoli Federico II, via Claudio 21, I-80125 Napoli, Italy. E-mail: [angelasara.cacciapuoti, gelli, paura, f.verde]@unina.it.

Publisher Item Identifier S 0000-0000(00)00000-3.

first contribution of this paper is to provide conditions on the spreading codes, which guarantee complete MAI rejection for WL-MUD in both underloaded and overloaded downlink configurations, when the DS-CDMA signal dominates the background noise. In particular, we will show that even the simple Walsh-Hadamard (WH) spreading codes can be suitably modified in order to fulfill such conditions.

Another limitation of almost all the performance studies carried out so far is the idealized assumption that the receivers are perfectly implemented. However, exception made for the WL decorrelating receiver, whose synthesis is data-independent, implementation of WL-MUD receivers requires knowledge of the second-order statistics (SOS) of the received signal $r(t)$, which can be estimated in practice from a finite number of samples. A theoretical performance analysis of the data-aided WL-MMSE and WL-MOE receivers was provided in [18], when the receivers are adaptively implemented by means of the least-mean square (LMS) algorithm, by evaluating the output signal-to-interference-plus-noise ratio (SINR). However, the SINR analysis carried out in [18] considers steady-state performances, i.e., when the sample size is infinite, and, thus, does not allow to evaluate the performance of the receivers as a function of the number of samples. This issue is important from a practical point of view because, especially when short sample-sizes are employed, the data-estimated versions of the WL-MUD receivers exhibit a severe performance degradation with respect to their ideal counterparts, reducing thus the expected performance gain over L-MUD receivers. To gain more insight about this point, this paper presents a finite-sample theoretical performance analysis of WL-MUD receivers, based on a first-order perturbative approach. In particular, taking as reference the WL-MOE receiver[1], two typical data-estimated implementations are considered: the WL-SMI (sample matrix inversion) receiver, which employs a sample estimate of the data autocorrelation matrix, and the WL-SUB (subspace) receiver, which exploits the properties of the eigenvalue decomposition (EVD) of the data autocorrelation matrix to reduce the effects of estimation errors. Finally, besides deriving accurate yet simple theoretical results for the finite-sample versions of the WL-MOE receivers, we will show that even some known results for the linear receivers must be reinterpreted or modified, to allow for a fair comparison between WL-MUD and L-MUD.

The paper is organized as follows. In Section II, we present the DS-CDMA system model and introduce the WL reception strategy. L-MOE and WL-MOE receivers are introduced in Section III, whereas Section IV analyzes their ideal performances, and derives simple conditions on the spreading codes, which assure perfect MAI suppression in the downlink. Section V presents the finite-sample performance analysis of the L-MOE and WL-MOE receivers. The theoretical results reported in Sections IV and V are validated and supported by computer simulations examples, whereas their proofs are gathered in Appendix I. Finally, concluding remarks are given in Section VI.

A. Notations

The fields of complex, real, and integer numbers are denoted with $\mathbb{C}$, $\mathbb{R}$, and $\mathbb{Z}$, respectively; matrices [vectors] are denoted with upper case [lower case] boldface letters (e.g., $\mathbf{A}$ or $\mathbf{a}$); the field of $m \times n$ complex [real] matrices is denoted as $\mathbb{C}^{m\times n}$ [$\mathbb{R}^{m\times n}$], with $\mathbb{C}^m$ [$\mathbb{R}^m$] used as a shorthand for $\mathbb{C}^{m\times 1}$ [$\mathbb{R}^{m\times 1}$]; the superscripts $*$, T, H, -1 and $\dagger$ denote the conjugate, the transpose, the Hermitian (conjugate transpose), the inverse, and the Moore-Penrose generalized inverse [19] (pseudo-inverse) of a matrix, respectively; $\mathbf{0}_m \in \mathbb{R}^m$, $\mathbf{O}_{m\times n} \in \mathbb{R}^{m\times n}$ and $\mathbf{I}_m \in \mathbb{R}^{m\times m}$ denote the null vector, the null matrix, and the identity matrix, respectively; trace$(\cdot)$ and rank$(\cdot)$ represent the trace and the rank; $\mathcal{N}(\mathbf{A})$, $\mathcal{R}(\mathbf{A})$, and $\mathcal{R}^\perp(\mathbf{A})$ denote the null space, the range (column space), and the orthogonal complement of the column space of $\mathbf{A} \in \mathbb{C}^{m\times n}[\mathbb{R}^{m\times n}]$ in $\mathbb{C}^m[\mathbb{R}^m]$; for any $\mathbf{a} \in \mathbb{C}^m$, $\|\mathbf{a}\| \triangleq (\mathbf{a}^H\mathbf{a})^{1/2}$ denotes the Euclidean norm; $\mathbf{A} = \text{diag}(A_{11}, A_{22}, \ldots, A_{nn})$ is a diagonal matrix with elements A_{ii} on the main diagonal; E$[\cdot]$ denotes ensemble averaging, $i \triangleq \sqrt{-1}$ is the imaginary unit, and Re$[\cdot]$ and Im$[\cdot]$ denote the real and imaginary parts; throughout the paper, we occasionally use the simplified notations $\mathbf{a}_\mathrm{R} \triangleq \text{Re}[\mathbf{a}]$, $\mathbf{a}_\mathrm{I} \triangleq \text{Im}[\mathbf{a}]$, $\mathbf{A}_\mathrm{R} \triangleq \text{Re}[\mathbf{A}]$, and $\mathbf{A}_\mathrm{I} \triangleq \text{Im}[\mathbf{A}]$; δ_k denotes the Kronecker delta (i.e., $\delta_k = 1$ for $k = 0$, zero otherwise); for any stationary discrete-time random vector process $\mathbf{x}(k) \in \mathbb{C}^m$, we denote with $\mathbf{R}_{\mathbf{xx}} \triangleq \text{E}[\mathbf{x}(k)\,\mathbf{x}^H(k)] \in \mathbb{C}^{m\times m}$ and with $\mathbf{R}_{\mathbf{xx}^*} \triangleq \text{E}[\mathbf{x}(k)\,\mathbf{x}^T(k)] \in \mathbb{C}^{m\times m}$ the autocorrelation matrix and the conjugate correlation matrix, respectively ($\mathbf{R}_{\mathbf{xx}} \equiv \mathbf{R}_{\mathbf{xx}^*} \in \mathbb{R}^{m\times m}$ when $\mathbf{x}(k) \in \mathbb{R}^m$).

II. Problem formulation and WL reception techniques

Let us consider the baseband model of a DS-CDMA system with J users, employing short spreading codes with N/T chips/symbol. After chip-matched filtering, perfect time synchronization and sampling with rate N/T, the received vector $\mathbf{r}(k) \in \mathbb{C}^N$ collecting the N samples of the incoming signal in the interval $[k\,T, (k+1)\,T)$, with $k \in \mathbb{Z}$, can be written [4] as follows:[2]

$$\begin{aligned}\mathbf{r}(k) &= \sum_{j=1}^{J} \alpha_j\, e^{i\,\theta_j}\, \boldsymbol{\psi}_j\, b_j(k) + \mathbf{v}(k) = \boldsymbol{\Psi}\,\mathbf{A}\,\boldsymbol{\Theta}\,\mathbf{b}(k) + \mathbf{v}(k) \\ &= \boldsymbol{\Phi}\,\mathbf{b}(k) + \mathbf{v}(k)\,, \end{aligned} \tag{1}$$

where, with reference to the jth user, $\alpha_j > 0$ is the received amplitude (accounting for transmitted energy and channel propagation loss), $\theta_j \in [0, 2\pi)$ is a precoding phase (which is deliberately introduced at the transmitter and whose role will be clear in the sequel), $\boldsymbol{\psi}_j \in \mathbb{C}^N$ is the unit-norm signature (encompassing spreading code and channel

[1]Although we consider the WL-MOE receiver, since it lends to some simplifications in the analysis, the obtained results can be applied also to the WL-MMSE receiver, since it is well known that the MMSE and MOE approaches are equivalent [4] in terms of output SINR. Moreover, it is not difficult to extend our analysis to other categories of receivers.

[2]The considered signal model is appropriate when: (i) the users are synchronous; (ii) the user channels introduce only interchip interference [4] and negligible intersymbol interference (ISI). However, all the results derived herein can be extended with straightforward modifications to account for asynchronous users and/or channels with ISI.

propagation effects), and $b_j(k)$ is the transmitted symbol, whereas $\mathbf{v}(k) \in \mathbb{C}^N$ accounts for thermal noise. Moreover, in (1), we have defined $\mathbf{\Psi} \triangleq [\boldsymbol{\psi}_1, \boldsymbol{\psi}_2, \ldots, \boldsymbol{\psi}_J] \in \mathbb{C}^{N \times J}$, $\mathbf{A} \triangleq \text{diag}(\alpha_1, \alpha_2, \ldots, \alpha_J) \in \mathbb{R}^{J \times J}$, $\mathbf{\Theta} \triangleq \text{diag}(e^{i\,\theta_1}, e^{i\,\theta_2}, \ldots, e^{i\,\theta_J}) \in \mathbb{C}^{J \times J}$, $\mathbf{\Phi} \triangleq \mathbf{\Psi}\,\mathbf{A}\,\mathbf{\Theta} \in \mathbb{C}^{N \times J}$, and the symbol vector $\mathbf{b}(k) \triangleq [b_1(k), b_2(k), \ldots, b_J(k)]^T \in \mathbb{R}^J$. Finally, let $\mathbf{c}_j \triangleq [c_j(0), c_j(1), \ldots, c_j(N-1)]^T \in \mathbb{C}^N$ denote the spreading vector of the jth user and let $g_j(n)$ be the corresponding baseband chip rate discrete-time impulse response, under the assumption that $g_j(n)$ has order $L_{g_j} \ll N$, the signature $\boldsymbol{\psi}_j$ in (1) can be modeled [4] as

$$\boldsymbol{\psi}_j = \mathbf{G}_j\,\mathbf{c}_j\,, \tag{2}$$

where $\mathbf{G}_j \in \mathbb{C}^{N \times N}$ is a Toeplitz lower triangular matrix with first column $[g_j(0), g_j(1), \ldots, g_j(L_{g_j}), 0, \ldots, 0]^T$ and first row $[g_j(0), 0, \ldots, 0]^T$.

Throughout the paper, we will assume that: **(a1)** $\mathbf{b}(k)$ is a binary[3] *real* zero-mean random vector, whose entries are independent and identically distributed (i.i.d.) random variables assuming equiprobable values in $\{-1, 1\}$, with $\mathbf{b}(k_1)$ and $\mathbf{b}(k_2)$ statistically independent for $k_1 \neq k_2$; **(a2)** $\mathbf{v}(k)$ is a *complex proper* [5] zero-mean Gaussian random vector, independent from $\mathbf{b}(k)$, where $\mathbf{R}_{\mathbf{vv}} = \sigma_v^2\,\mathbf{I}_N$ and $\mathbf{R}_{\mathbf{vv}^*} = \mathbf{O}_{N \times N}$, with $\mathbf{v}(k_1)$ and $\mathbf{v}(k_2)$ statistically independent for $k_1 \neq k_2$. DS-CDMA systems with real $\mathbf{b}(k)$ have been considered in [7], [8], [9], [11]. Moreover, models similar to (1) arise also in other applications; in particular, the case of a real $\mathbf{b}(k)$ has been considered in array processing [20], block equalization [21], orthogonal frequency-division multiplexing (OFDM) [22], multicarrier (MC) CDMA systems [23], and multiple-input multiple-output (MIMO) systems [24]. Therefore, most results of our analysis can be extended with minor modifications also to other application areas employing WL reception techniques.

Under assumptions **(a1)** and **(a2)**, the minimum-error-probability detection of $\mathbf{b}(k)$ is based only on $\mathbf{r}(k)$ (*one-shot* detection), and is equivalent to the maximum-likelihood (ML) rule

$$\begin{aligned} \widehat{\mathbf{b}}(k) &= \underset{\mathbf{b}(k)\in\mathbb{R}^J}{\text{argmin}}\, \|\mathbf{r}(k) - \mathbf{\Phi}\,\mathbf{b}(k)\|^2 \\ &= \underset{\mathbf{b}(k)\in\mathbb{R}^J}{\text{argmax}} \left\{ 2\,\mathbf{b}^T(k)\,\text{Re}[\mathbf{\Phi}^H\mathbf{r}(k)] - \mathbf{b}^T(k)\mathbf{\Phi}^H\mathbf{\Phi}\,\mathbf{b}(k) \right\}. \end{aligned} \tag{3}$$

This equation shows that the real vector $\mathbf{x}_{\text{R}}(k) \triangleq \text{Re}[\mathbf{\Phi}^H\mathbf{r}(k)] \in \mathbb{R}^J$, containing the real parts of the matched filter outputs, is a sufficient statistic for recovering $\mathbf{b}(k)$; this was recognized in [25], and pointed out more recently in [9], [26], [27]. Unless matrix $\mathbf{\Phi}$ has some special structure (e.g, orthogonal columns), implementing ML detection entails a complexity that grows exponentially with the number of users J. Focusing on detection of user j, a common *suboptimal* detection strategy is to perform linear processing of $\mathbf{x}_{\text{R}}(k)$ by a weight vector $\widetilde{\mathbf{g}}_j \in \mathbb{R}^J$:

$$y_j(k) = \widetilde{\mathbf{g}}_j^T\,\mathbf{x}_{\text{R}}(k)\,, \tag{4}$$

followed by a sgn(x) nonlinearity to detect $b_j(k)$. The main drawback of (4) is that, similarly to the ML receiver, it requires knowledge of the entire matrix $\mathbf{\Phi}$, i.e., signatures, amplitudes and phases of all the users. However, by recalling that $\mathbf{x}_{\text{R}}(k) = \text{Re}[\mathbf{x}(k)] = \frac{1}{2}\,\mathbf{x}(k) + \frac{1}{2}\,\mathbf{x}^*(k)$, the filter defined by (4) can be equivalently expressed as $y_j(k) = \widetilde{\mathbf{g}}_j^T\,\mathbf{x}_{\text{R}}(k) = \frac{1}{2}\,\widetilde{\mathbf{g}}_j^T\,\mathbf{x}(k) + \frac{1}{2}\,\widetilde{\mathbf{g}}_j^T\,\mathbf{x}^*(k) = \frac{1}{2}\,\widetilde{\mathbf{g}}_j^T\mathbf{\Phi}^H\mathbf{r}(k) + \frac{1}{2}\,\widetilde{\mathbf{g}}_j^T\,\mathbf{\Phi}^T\mathbf{r}^*(k)$, which can be simply rewritten as

$$y_j(k) = \mathbf{f}_{j,1}^H\,\mathbf{r}(k) + \mathbf{f}_{j,2}^H\,\mathbf{r}^*(k) = \mathbf{f}_j^H\,\mathbf{z}(k)\,, \tag{5}$$

where $\mathbf{f}_j \triangleq [\mathbf{f}_{j,1}^T, \mathbf{f}_{j,2}^T]^T \in \mathbb{C}^{2N}$, with $\mathbf{f}_{j,1} \triangleq \frac{1}{2}\,\mathbf{\Phi}\,\widetilde{\mathbf{g}}_j \in \mathbb{C}^N$ and $\mathbf{f}_{j,2} \triangleq \frac{1}{2}\,\mathbf{\Phi}^*\,\widetilde{\mathbf{g}}_j \in \mathbb{C}^N$, and, moreover, $\mathbf{z}(k) = [\mathbf{r}^T(k), \mathbf{r}^H(k)]^T \in \mathbb{C}^{2N}$. Regarding $\mathbf{f}_{j,1}$ and $\mathbf{f}_{j,2}$ as free vectors to be optimized, it is apparent that filter (5) operates directly on the received vector $\mathbf{r}(k)$, without requiring knowledge of $\mathbf{\Phi}$. Eq. (5) defines a *WL transformation*, involving both $\mathbf{r}(k)$ and its complex conjugate $\mathbf{r}^*(k)$, whereas the associated complex transformation $\mathbf{z}(k) \to y_j(k)$ is *linear* with respect to (w.r.t.) $\mathbf{z}(k)$ and, hence, the synthesis of $\mathbf{f}_j$ is simplified by resorting to this "augmented" formulation. However, observe that the output of (5) is real only when $\mathbf{f}_{j,1} = \mathbf{f}_{j,2}^*$, which is a *nonlinear* constraint on $\mathbf{f}_j$ [which will be referred to as the *conjugate symmetry (CS) constraint* in the following] that must be necessarily incorporated in any optimization criterion if the equivalence between (4) and (5) has to be preserved. Nevertheless, with reference to the maximum SINR criterion adopted later on, we will show that such a constraint is automatically satisfied by the unconstrained solution, hence it does not complicate in practice the receiver synthesis. We will rely in the following on formulation (5), since it allows many advantages not only in the synthesis, but also in the performance analysis of the receivers. Note that, unlike (4), eq. (5) encompasses as a particular case the *linear* receiver $y_j(k) = \mathbf{g}_j^H\,\mathbf{r}(k)$, with $\mathbf{g}_j \in \mathbb{C}^N$, which can be obtained indeed by setting $\mathbf{f}_{j,1} = \mathbf{g}_j$ and $\mathbf{f}_{j,2} = \mathbf{0}_N$. The output of such a linear receiver is not necessarily real-valued, hence it cannot be equivalent to (4); in spite of this incongruence, it is commonly adopted in many detection problem modeled by (1), even when the vector $\mathbf{b}(k)$ is real-valued (see, e.g., [28]).

III. The WL-MOE and L-MOE receivers

The main goal of this section is to derive the WL-MOE receiver as a particular solution of the maximum SINR criterion. We start by reviewing briefly the L-MOE receiver, not only to put the necessary bases for our subsequent derivations, but also to comment on possible inconsistencies concerning the "correct" definition of the SINR to be used for linear receivers, when real symbols are employed.

In order to recover $b_j(k)$ by a linear receiver, it is useful to rewrite (1) as follows:

$$\mathbf{r}(k) = \boldsymbol{\phi}_j\,b_j(k) + \overline{\mathbf{\Phi}}_j\,\overline{\mathbf{b}}_j(k) + \mathbf{v}(k) = \boldsymbol{\phi}_j\,b_j(k) + \mathbf{p}_j(k)\,, \tag{6}$$

[3] This assumption is not crucial, but simplifies the analysis. Our derivations can be readily extended to the case where the entries of $\mathbf{b}(k)$ assume values in an *arbitrary* real set, or even when the entries of $\mathbf{b}(k)$ are not real but obey the more general *conjugate symmetry* [20] property.

where $\boldsymbol{\phi}_j \in \mathbb{C}^N$ is the jth column of the composite matrix $\boldsymbol{\Phi}$, whereas $\overline{\mathbf{b}}_j(k) \in \mathbb{R}^{J-1}$ denotes the vector that includes all the elements of $\mathbf{b}(k)$ except for the jth entry $b_j(k)$, $\overline{\boldsymbol{\Phi}}_j \in \mathbb{C}^{N\times(J-1)}$ denotes the matrix that includes all the columns of $\boldsymbol{\Phi}$ except for the jth column $\boldsymbol{\phi}_j$, and, finally, $\mathbf{p}_j(k) \triangleq \overline{\boldsymbol{\Phi}}_j\,\overline{\mathbf{b}}_j(k) + \mathbf{v}(k) \in \mathbb{C}^N$ is the interference-plus-noise (disturbance) vector. Accounting for (6), the output of a linear receiver can be expressed as

$$y_j(k) = \mathbf{g}_j^H \mathbf{r}(k) = \mathbf{g}_j^H \boldsymbol{\phi}_j\, b_j(k) + \mathbf{g}_j^H \mathbf{p}_j(k)\,. \tag{7}$$

The L-MOE receiver [4] is the solution of the following constrained optimization problem:

$$\mathbf{g}_{j,\text{L-MOE}} = \underset{\mathbf{g}_j \in \mathbb{C}^N}{\operatorname{argmin}}\, \mathrm{E}[|y_j(k)|^2] \quad \text{subject to } \mathbf{g}_j^H\, \boldsymbol{\phi}_j = 1\,, \tag{8}$$

which can be solved by Lagrange optimization, yielding the two equivalent[4] expressions

$$\begin{aligned}\mathbf{g}_{j,\text{L-MOE}} &= (\boldsymbol{\phi}_j^H \mathbf{R}_{\mathbf{rr}}^{-1} \boldsymbol{\phi}_j)^{-1}\, \mathbf{R}_{\mathbf{rr}}^{-1}\, \boldsymbol{\phi}_j \\ &= (\boldsymbol{\phi}_j^H \mathbf{R}_{\mathbf{p}_j\mathbf{p}_j}^{-1} \boldsymbol{\phi}_j)^{-1}\, \mathbf{R}_{\mathbf{p}_j\mathbf{p}_j}^{-1}\, \boldsymbol{\phi}_j\,,\end{aligned} \tag{9}$$

where the second equality follows by applying the matrix inversion lemma[5] to the autocorrelation matrix $\mathbf{R}_{\mathbf{rr}} = \boldsymbol{\phi}_j\boldsymbol{\phi}_j^H + \mathbf{R}_{\mathbf{p}_j\mathbf{p}_j}$. It can be easily shown that, among all linear receivers, the L-MOE one maximizes the SINR at its output, which, accounting for (7), can be defined as

$$\begin{aligned}\overline{\text{SINR}}(\mathbf{g}_j) &\triangleq \frac{\mathrm{E}[|\mathbf{g}_j^H \boldsymbol{\phi}_j\, b_j(k)|^2]}{\mathrm{E}[|\mathbf{g}_j^H \mathbf{p}_j(k)|^2]} = \frac{|\mathbf{g}_j^H \boldsymbol{\phi}_j|^2}{\mathbf{g}_j^H \mathbf{R}_{\mathbf{p}_j\mathbf{p}_j}\, \mathbf{g}_j} \\ &= \frac{|(\mathbf{R}_{\mathbf{p}_j\mathbf{p}_j}^{1/2}\, \mathbf{g}_j)^H (\mathbf{R}_{\mathbf{p}_j\mathbf{p}_j}^{-1/2} \boldsymbol{\phi}_j)|^2}{\|\mathbf{R}_{\mathbf{p}_j\mathbf{p}_j}^{1/2}\, \mathbf{g}_j\|^2}\,.\end{aligned} \tag{10}$$

Indeed, by using the Cauchy-Schwartz's inequality[6], any receiver maximizing (10) is given by $\mathbf{g}_{j,\text{max-SINR}} = \gamma_j\, \mathbf{R}_{\mathbf{p}_j\mathbf{p}_j}^{-1}\, \boldsymbol{\phi}_j$, where $\gamma_j \in \mathbb{C} - \{0\}$ is an arbitrary (nonnull) complex scalar. Hence, the L-MOE receiver is obtained by setting $\gamma_j = (\boldsymbol{\phi}_j^H \mathbf{R}_{\mathbf{p}_j\mathbf{p}_j}^{-1} \boldsymbol{\phi}_j)^{-1}$, and the maximum value of (10) is

$$\begin{aligned}\overline{\text{SINR}}_{j,\max} &\triangleq \overline{\text{SINR}}(\mathbf{g}_{j,\text{L-MOE}}) = \frac{1}{\mathbf{g}_{j,\text{L-MOE}}^H\, \mathbf{R}_{\mathbf{p}_j\mathbf{p}_j}\, \mathbf{g}_{j,\text{L-MOE}}} \\ &= \boldsymbol{\phi}_j^H \mathbf{R}_{\mathbf{p}_j\mathbf{p}_j}^{-1} \boldsymbol{\phi}_j\,.\end{aligned} \tag{11}$$

Turning to the WL-MOE receiver, we preliminarily express $\mathbf{z}(k)$, defined in (5), as

$$\mathbf{z}(k) = \mathbf{H}\,\mathbf{b}(k) + \mathbf{d}(k)\,, \tag{12}$$

where $\mathbf{H} \triangleq [\boldsymbol{\Phi}^T, \boldsymbol{\Phi}^H]^T \in \mathbb{C}^{2N\times J}$ and $\mathbf{d}(k) \triangleq [\mathbf{v}^T(k), \mathbf{v}^H(k)]^T \in \mathbb{C}^{2N}$. Accounting for **(a2)**, the noise $\mathbf{d}(k)$ is an *improper* Gaussian random vector, with $\mathbf{R}_{\mathbf{dd}} = \sigma_v^2\, \mathbf{I}_{2N}$ and $\mathbf{R}_{\mathbf{dd}^*} = \sigma_v^2\, \mathbf{J}_{2N}$, where

$$\mathbf{J}_{2N} \triangleq \begin{bmatrix} \mathbf{O}_{N\times N} & \mathbf{I}_N \\ \mathbf{I}_N & \mathbf{O}_{N\times N} \end{bmatrix} \in \mathbb{R}^{2N\times 2N} \tag{13}$$

is a block permutation matrix [29]. Accounting for (12), eq. (5) can be written as

$$\begin{aligned}y_j(k) &= \mathbf{f}_j^H \mathbf{h}_j\, b_j(k) + \mathbf{f}_j^H [\overline{\mathbf{H}}_j\, \overline{\mathbf{b}}_j(k) + \mathbf{d}(k)] \\ &= \mathbf{f}_j^H \mathbf{h}_j\, b_j(k) + \mathbf{f}_j^H\, \mathbf{q}_j(k)\,,\end{aligned} \tag{14}$$

where $\mathbf{h}_j = [\boldsymbol{\phi}_j^T, \boldsymbol{\phi}_j^H]^T \in \mathbb{C}^{2N}$, $\overline{\mathbf{H}}_j = [\overline{\boldsymbol{\Phi}}_j^T, \overline{\boldsymbol{\Phi}}_j^H]^T \in \mathbb{C}^{2N\times(J-1)}$, and $\mathbf{q}_j(k) \triangleq [\mathbf{p}_j^T(k), \mathbf{p}_j^H(k)]^T = \overline{\mathbf{H}}_j\, \overline{\mathbf{b}}_j(k) + \mathbf{d}(k) \in \mathbb{C}^{2N}$ is the augmented disturbance vector. To establish a general framework encompassing both linear and WL receivers, we refer to the scheme in Fig. 1, wherein linear receivers can be obtained by setting $\mathbf{f}_{j,2} = \mathbf{0}_N$, and the $\mathrm{Re}[\cdot]$ operation is needed only when $y_j(k)$ is complex, as it happens for linear receivers, or even for WL ones possibly not satisfying the CS constraint. It should be observed that the L-MOE receiver maximizes the $\overline{\text{SINR}}$ given by (10), which is evaluated *before* the $\mathrm{Re}[\cdot]$ block. Since $b_j(k)$ is real, a more appropriate performance measure is the SINR *after* the $\mathrm{Re}[\cdot]$ block, which can be written, accounting for (14), as

$$\text{SINR}(\mathbf{f}_j) \triangleq \frac{\mathrm{E}\{\mathrm{Re}^2[\mathbf{f}_j^H \mathbf{h}_j\, b_j(k)]\}}{\mathrm{E}\{\mathrm{Re}^2[\mathbf{f}_j^H \mathbf{q}_j(k)]\}} = \frac{\mathrm{Re}^2[\mathbf{f}_j^H \mathbf{h}_j]}{\mathrm{E}\{\mathrm{Re}^2[\mathbf{f}_j^H \mathbf{q}_j(k)]\}} \tag{15}$$

Indeed, if the disturbance contribution $\mathbf{f}_j^H\, \mathbf{q}_j(k)$ at the receiver output can be approximated as a Gaussian random variable[7], maximizing (15) w.r.t $\mathbf{f}_j$ amounts to minimizing the error probability $P_{e,j} \triangleq \Pr\{\hat{b}_j(k) \neq b_j(k)\} \approx Q(\sqrt{\text{SINR}(\mathbf{f}_j)})$, where $Q(x) \triangleq (1/\sqrt{2\pi}) \int_x^{+\infty} e^{-u^2/2}\, du$ denotes the Q function. Since maximization of (15), due to the presence of the $\mathrm{Re}[\cdot]$ operator, is not as standard as maximizing (10), we discuss it briefly in the following Lemma.

Lemma 1: Any WL receiver (5) maximizing (15) can be expressed as

$$\mathbf{f}_{j,\text{max-SINR}} = \xi_j\, \mathbf{R}_{\mathbf{q}_j\mathbf{q}_j}^{-1}\, \mathbf{h}_j + \mathbf{f}_{j,\text{a}}\,, \tag{16}$$

where $\xi_j \in \mathbb{R} - \{0\}$ is an arbitrary (nonnull) real scalar and $\mathbf{f}_{j,\text{a}}$ is an arbitrary antisymmetric vector, i.e., $\mathbf{f}_{j,\text{a}} \in \mathcal{A} \triangleq \{\mathbf{f} =$

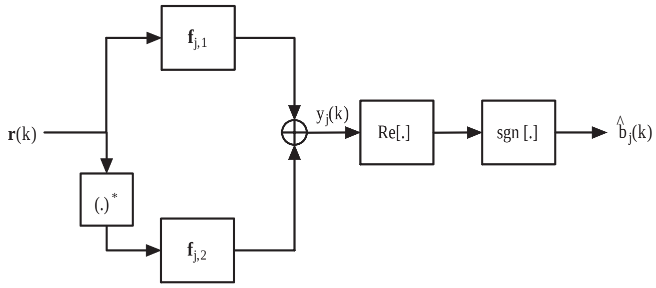

Fig. 1. The WL processing scheme.

[4]The advantage of using $\mathbf{R}_{\mathbf{rr}}$ instead of $\mathbf{R}_{\mathbf{p}_j\mathbf{p}_j}$ in (9) is that the former can be estimated from received data.

[5]Given the vectors $\mathbf{x}, \mathbf{y} \in \mathbb{C}^n$ and the nonsingular matrix $\mathbf{X} \in \mathbb{C}^{n\times n}$, the matrix inversion lemma states that $(\mathbf{X} + \mathbf{x}\,\mathbf{y}^H)^{-1} = \mathbf{X}^{-1} - (1 + \mathbf{y}^H\, \mathbf{X}^{-1}\, \mathbf{x})^{-1} \mathbf{X}^{-1}\, \mathbf{x}\, \mathbf{y}^H\, \mathbf{X}^{-1}$.

[6]Given the vectors $\mathbf{x}, \mathbf{y} \in \mathbb{C}^n$, the Cauchy-Schwartz's inequality states that $|\mathbf{x}^H \mathbf{y}|^2 \leq \|\mathbf{x}\|^2 \|\mathbf{y}\|^2$, where the upper bound is achieved by $\mathbf{y} = \gamma\, \mathbf{x}$, with $\gamma \in \mathbb{C}$.

[7]When N and J are large enough, this assumption is well-satisfied for maximum-SINR equalizers (see, e.g, [30]).

$[\mathbf{f}_1^T, \mathbf{f}_2^T]^T \in \mathbb{C}^{2N} \,|\, \mathbf{f}_1 = -\mathbf{f}_2^* \in \mathbb{C}^N\}$. The resulting maximum SINR is given by

$$\text{SINR}_{j,\text{max}} \triangleq \text{SINR}(\mathbf{f}_{j,\text{max-SINR}}) = \mathbf{h}_j^H \mathbf{R}_{\mathbf{q}_j\mathbf{q}_j}^{-1} \mathbf{h}_j \,. \tag{17}$$

Proof: See Appendix A. ∎

Note that the maximum SINR solution (16) differs from that of the linear case for the fact that the scalar ξ_j must be real and for the presence of the antisymmetric vector $\mathbf{f}_{j,\text{a}}$. Moreover, in Appendix A it is also shown that the value of SINR (15) does not depend on $\xi_j \in \mathbb{R} - \{0\}$ and on $\mathbf{f}_{j,\text{a}}$. Hence, we can choose ξ_j such that $\mathbf{f}_{j,\text{max-SINR}}^H \mathbf{h}_j = 1$ and $\mathbf{f}_{j,\text{a}} = \mathbf{0}_{2N}$, which leads to the WL-MOE receiver:

$$\begin{aligned}\mathbf{f}_{j,\text{WL-MOE}} &= (\mathbf{h}_j^H \mathbf{R}_{\mathbf{zz}}^{-1} \mathbf{h}_j)^{-1} \mathbf{R}_{\mathbf{zz}}^{-1} \mathbf{h}_j \\ &= (\mathbf{h}_j^H \mathbf{R}_{\mathbf{q}_j\mathbf{q}_j}^{-1} \mathbf{h}_j)^{-1} \mathbf{R}_{\mathbf{q}_j\mathbf{q}_j}^{-1} \mathbf{h}_j \,,\end{aligned} \tag{18}$$

where the second equality[8] follows by applying the matrix inversion lemma (see footnote 5) to the autocorrelation matrix $\mathbf{R}_{\mathbf{zz}} = \mathbf{h}_j \mathbf{h}_j^H + \mathbf{R}_{\mathbf{q}_j\mathbf{q}_j}$. By reasoning as in the proof of Lemma 1, it can be shown that (18) is obtained equivalently as the unique solution of the following WL-MOE criterion:

$$\mathbf{f}_{j,\text{WL-MOE}} = \underset{\mathbf{f}_j \in \mathbb{C}^{2N}}{\operatorname{argmin}} \, \text{E}\{\text{Re}^2[y_j(k)]\} \;\; \text{subject to } \mathbf{f}_j^H \mathbf{h}_j = 1 \,. \tag{19}$$

IV. Ideal performances of the L-MOE and WL-MOE receivers

In this section, we compare the SINR performances of the *ideal* WL-MOE and the L-MOE receivers, i.e., those receivers whose synthesis is based on perfect knowledge of the SOS of the received signal. The analysis for the data-estimated versions of the receivers will be carried out in Section V.

In order to carry out a meaningful performance comparison between linear and WL receivers, following [18], we evaluate for both receivers the SINR *after* the Re$[\cdot]$ block, given by (15). Since the WL-MOE receiver maximizes such a SINR (see Lemma 1), one simply has:

$$\text{SINR}_{j,\text{WL-MOE}} \triangleq \text{SINR}(\mathbf{f}_{j,\text{WL-MOE}}) = \mathbf{h}_j^H \, \mathbf{R}_{\mathbf{q}_j\mathbf{q}_j}^{-1} \, \mathbf{h}_j \,. \tag{20}$$

Instead, observe that evaluating the SINR given by (15) for the L-MOE receiver leads to a result generally different from (11). By observing that the L-MOE receiver can be viewed as a WL receiver with augmented weight vector $\mathbf{f}_{j,\text{L-MOE}} \triangleq [\mathbf{g}_{j,\text{L-MOE}}^T, \mathbf{0}_N^T]^T$, recalling that $\mathbf{g}_{j,\text{L-MOE}}^H \, \boldsymbol{\phi}_j = 1$, and applying the straightforward identity $\text{Re}^2[z] = \frac{1}{2}\{|z|^2 + \text{Re}[z^2]\}$, $\forall z \in \mathbb{C}$, the SINR (15) for the L-MOE receiver can be written as

$$\begin{aligned}\text{SINR}_{j,\text{L-MOE}} &\triangleq \text{SINR}(\mathbf{f}_{j,\text{L-MOE}}) = \frac{1}{\text{E}\{\text{Re}^2[\mathbf{g}_{j,\text{L-MOE}}^H \mathbf{p}_j(k)]\}} \\ &= \frac{2}{\mathbf{g}_{j,\text{L-MOE}}^H \mathbf{R}_{\mathbf{p}_j\mathbf{p}_j} \mathbf{g}_{j,\text{L-MOE}} + \text{Re}[\mathbf{g}_{j,\text{L-MOE}}^H \mathbf{R}_{\mathbf{p}_j\mathbf{p}_j^*} \mathbf{g}_{j,\text{L-MOE}}^*]} \,.\end{aligned} \tag{21}$$

On one hand, since the WL-MOE is a maximum-SINR receiver, it results that $\text{SINR}_{j,\text{L-MOE}} \leq \text{SINR}_{j,\text{WL-MOE}}$. On the other hand, since $\text{Re}^2[z] \leq |z|^2$, $\forall z \in \mathbb{C}$, accounting for (11), one has $\text{SINR}_{j,\text{L-MOE}} \geq \overline{\text{SINR}}_{j,\text{max}}$. Overall, we maintain that

$$\text{SINR}_{j,\text{WL-MOE}} \geq \text{SINR}_{j,\text{L-MOE}} \geq \overline{\text{SINR}}_{j,\text{max}} \,. \tag{22}$$

Although the first inequality in (22) concisely states that the performance of the WL-MOE receiver is not worse than that of its linear counterpart, it does not allow us to quantify the relative performance gain. Indeed, no clear insight on the performance comparison between the WL-MOE and L-MOE receivers can be drawn out from the SINR formulas (20) and (21). To overcome this conceptual difficulty, we carry out in the next subsection the performance comparison in the high-SNR regime, by deriving the analytical expressions of $\text{SINR}_{j,\text{WL-MOE}}$ and $\text{SINR}_{j,\text{L-MOE}}$ as the noise variance σ_v^2 approaches zero. It should be observed that, more generally, the results reported in Subsection IV-A turn out to be useful in all those situations wherein the DS-CDMA signal dominates the background noise, which is a common occurrence in many practical environments.

A. Analysis in the high-SNR regime

The discussion carried out in this subsection is mainly based on some mathematical results whose proofs are reported in Appendix B. Such results show that, in the limiting case of vanishingly small noise, i.e., as $\sigma_v^2 \to 0$, the performance comparison between the L-MOE and WL-MOE receivers heavily depends on the rank properties of $\mathbf{\Phi}$ and $\mathbf{H}$, respectively.

As regards linear processing, it is shown that, in the high-SNR regime, the L-MOE receiver is able to achieve perfect MAI suppression for *each* active user, that is, $\lim_{\sigma_v^2 \to 0} \text{SINR}_{j,\text{L-MOE}} = \lim_{\sigma_v^2 \to 0} \overline{\text{SINR}}_{j,\text{max}} = +\infty$, $\forall j \in \{1, 2, \ldots, J\}$, if and only if (iff) the matrix $\mathbf{\Phi}$ is full-column rank, i.e., $\text{rank}(\mathbf{\Phi}) = J$. Moreover, in such a case, it results that

$$\lim_{\sigma_v^2 \to 0} \frac{\text{SINR}_{j,\text{L-MOE}}}{\overline{\text{SINR}}_{j,\text{max}}} = 2 \,, \quad \forall j \in \{1, 2, \ldots, J\} \,, \tag{23}$$

which shows that, as intuitively expected, since the Re$[\cdot]$ block in Fig. 1 discards one-half of the noise-plus-MAI power in $y_j(k)$, $\text{SINR}_{j,\text{L-MOE}}$ is asymptotically greater than $\overline{\text{SINR}}_{j,\text{max}}$ of exactly 3 dB. Note that this simple result holds only when $\text{rank}(\mathbf{\Phi}) = J$. If the matrix $\mathbf{\Phi}$ is not full-column rank, the L-MOE receiver is unable to perfectly suppress the MAI, even in the absence of noise; in this case, both $\overline{\text{SINR}}_{j,\text{max}}$ and $\text{SINR}_{j,\text{L-MOE}}$ take on finite values, which depend on $\boldsymbol{\phi}_j$ and the eigenstructure of the MAI autocorrelation matrix $\overline{\mathbf{\Phi}}_j \overline{\mathbf{\Phi}}_j^H$. Therefore, the assumption $\text{rank}(\mathbf{\Phi}) = J$ is crucial and deserves a brief comment. By virtue of nonsingularity of the diagonal matrices $\mathbf{A}$ and $\mathbf{\Theta}$, it follows that $\text{rank}(\mathbf{\Phi}) = \text{rank}(\mathbf{\Psi}\,\mathbf{A}\,\mathbf{\Theta}) = \text{rank}(\mathbf{\Psi})$. Henceforth, the matrix $\mathbf{\Phi}$ is full-column rank iff the signatures $\boldsymbol{\psi}_1, \boldsymbol{\psi}_2, \ldots, \boldsymbol{\psi}_J$ are linearly independent, a condition which can be fulfilled only if the number of users J is smaller than or equal to the processing gain N (underloaded systems). It is noteworthy that the linear independence of the signatures $\boldsymbol{\psi}_1, \boldsymbol{\psi}_2, \ldots, \boldsymbol{\psi}_J$ depends on both the spreading codes and the channel impulse responses of all the active users. Thus, in general, it is difficult to give

[8]The advantage of using $\mathbf{R}_{\mathbf{zz}}$ instead of $\mathbf{R}_{\mathbf{q}_j\mathbf{q}_j}$ in (18) is that the former can be estimated from received data.

easily interpretable conditions assuring that $\boldsymbol{\Psi}$ is full-column rank. A substantial simplification occurs in the downlink, wherein all the user signals propagate through a common multipath channel, i.e., $g_j(n) = g(n)$, with order $L_{g_j} = L_g$, for each user. In this case, the signature $\boldsymbol{\psi}_j$ given by (2) becomes $\boldsymbol{\psi}_j = \mathbf{G}\,\mathbf{c}_j$, where the common Toeplitz channel matrix $\mathbf{G} = \mathbf{G}_j$ turns out to be nonsingular under the mild assumption that $g(0) \neq 0$, which is assumed to hold hereinafter. Accounting for this model, the matrix $\boldsymbol{\Psi}$ becomes

$$\boldsymbol{\Psi} = \mathbf{G}\,\underbrace{[\mathbf{c}_1, \mathbf{c}_2, \ldots, \mathbf{c}_J]}_{\mathbf{C}\in\mathbb{C}^{N\times J}} = \mathbf{G}\,\mathbf{C}\,, \tag{24}$$

which, by virtue of nonsingularity of $\mathbf{G}$, implies that $\text{rank}(\boldsymbol{\Phi}) = \text{rank}(\boldsymbol{\Psi}) = \text{rank}(\mathbf{C})$. Consequently, in the downlink scenario, the linear independence of the spreading vectors $\mathbf{c}_1, \mathbf{c}_2, \ldots, \mathbf{c}_J$ is a necessary and sufficient condition for assuring the full-column rank property of $\boldsymbol{\Phi}$ and, hence, allowing the L-MOE receiver to completely reject the MAI in the high-SNR region. Let us focus attention on the performance comparison between the L-MOE and WL-MOE receivers. As a first result, it is shown in Appendix B that, if $\boldsymbol{\Phi}$ (or, equivalently, $\boldsymbol{\Psi}$) is full-column rank, then

$$\lim_{\sigma_v^2\to 0} \frac{\text{SINR}_{j,\text{WL-MOE}}}{\text{SINR}_{j,\text{L-MOE}}} = \frac{\|\boldsymbol{\phi}_j\|^2 - \text{Re}[\boldsymbol{\phi}_j^H \overline{\boldsymbol{\Phi}}_j]\{\text{Re}[\overline{\boldsymbol{\Phi}}_j^H \overline{\boldsymbol{\Phi}}_j]\}^{-1}\text{Re}[\overline{\boldsymbol{\Phi}}_j^H \boldsymbol{\phi}_j]}{\|\boldsymbol{\phi}_j\|^2 - \boldsymbol{\phi}_j^H \overline{\boldsymbol{\Phi}}_j(\overline{\boldsymbol{\Phi}}_j^H \overline{\boldsymbol{\Phi}}_j)^{-1}\overline{\boldsymbol{\Phi}}_j^H \boldsymbol{\phi}_j}\,, \tag{25}$$

which, in addition to (22), evidences that, since $\lim_{\sigma_v^2\to 0} \text{SINR}_{j,\text{L-MOE}} = +\infty$ when $\text{rank}(\boldsymbol{\Phi}) = J$, the WL-MOE receiver also suppresses the MAI exactly in the high-SNR regime, i.e., $\lim_{\sigma_v^2\to 0} \text{SINR}_{j,\text{WL-MOE}} = +\infty$, $\forall j \in \{1, 2, \ldots, J\}$. Remarkably, it is apparent from (25) that, if

$$\text{Re}[\boldsymbol{\phi}_j^H \overline{\boldsymbol{\Phi}}_j]\,\{\text{Re}[\overline{\boldsymbol{\Phi}}_j^H \overline{\boldsymbol{\Phi}}_j]\}^{-1}\,\text{Re}[\overline{\boldsymbol{\Phi}}_j^H \boldsymbol{\phi}_j] = \boldsymbol{\phi}_j^H \overline{\boldsymbol{\Phi}}_j\,(\overline{\boldsymbol{\Phi}}_j^H \overline{\boldsymbol{\Phi}}_j)^{-1}\,\overline{\boldsymbol{\Phi}}_j^H \boldsymbol{\phi}_j\,, \tag{26}$$

we have:

$$\lim_{\sigma_v^2\to 0} \frac{\text{SINR}_{j,\text{WL-MOE}}}{\text{SINR}_{j,\text{L-MOE}}} = 1\,, \tag{27}$$

which renders the L-MOE and WL-MOE receivers perfectly equivalent in terms of SINR, as $\sigma_v^2 \to 0$. In other words, if $\boldsymbol{\Phi}$ is full-column rank (as may be the case in underloaded systems) and condition (26) is fulfilled, WL processing does not improve upon conventional linear processing in the high-SNR region. It is interesting to observe that, for instance, condition (26) is trivially satisfied if $\boldsymbol{\phi}_j$ and $\overline{\boldsymbol{\Phi}}_j$ are real (i.e., matrix $\boldsymbol{\Phi}$ is real), or when the user signatures are orthogonal[9], i.e., $\boldsymbol{\psi}_{j_1}^H \boldsymbol{\psi}_{j_2} = 0$, $\forall j_1 \neq j_2 \in \{1, 2, \ldots, J\}$, independently of matrices $\mathbf{A}$ and $\boldsymbol{\Theta}$ [see (1)]. To gain further insight about (25), we consider the two-users case (i.e., $J = 2$), and, without loss of generality, we assume that the desired user is the first one (i.e., $j = 1$). In this case, eq. (25) simplifies to

$$\lim_{\sigma_v^2\to 0} \frac{\text{SINR}_{1,\text{WL-MOE}}}{\text{SINR}_{1,\text{L-MOE}}} = \frac{1 - |\rho|^2\cos^2(\Delta\theta - \measuredangle\rho)}{1 - |\rho|^2}\,, \tag{28}$$

which suggests that the performance advantage of the WL-MOE receiver over the L-MOE one depends on the magnitude $|\rho|$ and phase $\measuredangle\rho$ of the correlation coefficient $\rho \triangleq \boldsymbol{\psi}_1^H \boldsymbol{\psi}_2$ between the two signatures $\boldsymbol{\psi}_1$ and $\boldsymbol{\psi}_2$, as well as on the phase difference $\Delta\theta \triangleq \theta_1 - \theta_2$. This is in accordance with the results derived in [16] in terms of near-far resistance. Specifically, for a given value of $0 < |\rho| < 1$, the largest performance gap between WL-MOE and L-MOE receivers is obtained when $\Delta\theta - \measuredangle\rho = \pi/2 + h\,\pi$, with $h \in \mathbb{Z}$, whereas the two receivers achieve the same performance when $\Delta\theta - \measuredangle\rho = h\,\pi$, independently of the value of $|\rho|$. On the other hand, for a given value of $\Delta\theta - \measuredangle\rho \neq h\,\pi$, the performance gain of the WL-MOE receiver over the L-MOE one increases without bounds, as the magnitude of ρ approaches unity, i.e., the user signatures are maximally correlated.

As a second result, it is evidenced in Appendix B that, contrary to the L-MOE receiver, the WL-MOE one is able to ensure perfect MAI suppression in the high-SNR regime, even when the number of users J exceeds the processing gain N (overloaded systems). Indeed, it is shown that, more generally, $\lim_{\sigma_v^2\to 0} \text{SINR}_{j,\text{WL-MOE}} = +\infty$, $\forall j \in \{1, 2, \ldots, J\}$, iff $\mathbf{H}$ is full-column rank. If $\boldsymbol{\Phi}$ is full-column rank (a condition that can hold only when the system is underloaded), then $\mathbf{H}$ is full-column rank, too. However, the matrix $\mathbf{H}$ can be full-column rank even when $N < J \leq 2\,N$, wherein $\boldsymbol{\Phi}$ is structurally rank-deficient; in this overloaded environment, it results that

$$\lim_{\sigma_v^2\to 0} \frac{\text{SINR}_{j,\text{WL-MOE}}}{\text{SINR}_{j,\text{L-MOE}}} = +\infty\,, \quad \forall j \in \{1, 2, \ldots, J\}\,. \tag{29}$$

In other words, provided that $\text{rank}(\mathbf{H}) = J$, the performance gap between the WL-MOE and L-MOE receivers becomes arbitrarily large for vanishingly small noise, when $N < J \leq 2\,N$. This fact strongly motivates us to provide conditions assuring that $\mathbf{H}$ be full-column rank in overloaded scenarios. To this aim, we provide the following Theorem, by focusing attention directly on the downlink scenario in an effort to give simple and insightful conditions.

Theorem 1: When $N < J \leq 2\,N$, the code matrix can be decomposed as $\mathbf{C} = \mathbf{C}_{\text{left}}\,[\mathbf{I}_N\ \boldsymbol{\Pi}]$, where $\mathbf{C}_{\text{left}} \triangleq [\mathbf{c}_1,\ \mathbf{c}_2, \ldots, \mathbf{c}_N] \in \mathbb{C}^{N\times N}$ is nonsingular and $\boldsymbol{\Pi} \in \mathbb{C}^{N\times(J-N)}$ is a tall matrix. In this overloaded scenario, under the assumption that $\boldsymbol{\Psi}$ exhibits the form given by (24), the matrix $\mathbf{H}$ is full-column rank iff $\boldsymbol{\Pi}^* - (\boldsymbol{\Theta}_1^2)^*\,\boldsymbol{\Pi}\,\boldsymbol{\Theta}_2^2 \in \mathbb{C}^{N\times(J-N)}$ is full-column rank, where $\boldsymbol{\Theta}_1 \triangleq \text{diag}(e^{i\,\theta_1}, e^{i\,\theta_2}, \ldots, e^{i\,\theta_N}) \in \mathbb{C}^{N\times N}$ and $\boldsymbol{\Theta}_2 \triangleq \text{diag}(e^{i\,\theta_{N+1}}, e^{i\,\theta_{N+2}}, \ldots, e^{i\,\theta_J}) \in \mathbb{C}^{(J-N)\times(J-N)}$.

Proof: See Appendix C. ■

Theorem 1 deserves some interesting comments, aimed at clarifying in particular the role of the precoding phases in (1), which are at the designer's disposal. First of all, it is apparent that the full-column rank property of $\mathbf{H}$ does not depend

[9]As a matter of fact, if the user signatures are orthogonal, under assumptions **(a1)** and **(a2)**, the single-user detector, which simply matches the received vector $\mathbf{r}(k)$ to $\boldsymbol{\phi}_j$, is indeed the optimal (in the minimum-error-probability sense) receiver.

on the channel impulse response[10], but depends on both the spreading codes of all the active users and their precoding phases $\theta_1, \theta_2, \ldots, \theta_J$. To this respect, it is interesting to investigate how such phases influence the full-column rank property of $\mathbf{H}$ in overloaded systems, focusing attention to the case wherein Walsh-Hadamard (WH) spreading codes are employed. To do this, without loss of generality, assume that $\mathbf{c}_{N+j} = \mathbf{c}_j$, for $j \in \{1, 2, \ldots, J-N\}$, and let $\mathbf{C}_{\text{left}}$ denote the common Hadamard matrix of order N. In this case, it is easily verified that $\mathbf{\Pi} = [\mathbf{e}_1, \mathbf{e}_2, \ldots, \mathbf{e}_{J-N}]$, with $\mathbf{e}_j$ denoting the jth column of $\mathbf{I}_N$. Thus, if WH spreading vectors are used, the matrix $\mathbf{\Pi}$ is real-valued (i.e., $\mathbf{\Pi} = \mathbf{\Pi}^*$) and, moreover, one has $(\mathbf{\Theta}_1^2)^* \, \mathbf{\Pi} = \mathbf{\Pi} \, (\mathbf{\Theta}_{1,\text{red}}^2)^*$, where $\mathbf{\Theta}_{1,\text{red}} \triangleq \text{diag}(e^{i\,\theta_1}, e^{i\,\theta_2}, \ldots, e^{i\,\theta_{J-N}}) \in \mathbb{C}^{(J-N)\times(J-N)}$. In light of these observations, by additionally remembering that $\mathbf{\Pi}$ is full-column rank, it follows that $\text{rank}[\mathbf{\Pi}^* - (\mathbf{\Theta}_1^2)^* \, \mathbf{\Pi} \, \mathbf{\Theta}_2^2] = \text{rank}\{\mathbf{\Pi} \, [\mathbf{I}_{J-N} - (\mathbf{\Theta}_{1,\text{red}}^2)^* \, \mathbf{\Theta}_2^2]\} = \text{rank}[\mathbf{I}_{J-N} - (\mathbf{\Theta}_{1,\text{red}}^2)^* \, \mathbf{\Theta}_2^2]$. Since the matrix $\mathbf{I}_{J-N} - (\mathbf{\Theta}_{1,\text{red}}^2)^* \, \mathbf{\Theta}_2^2$ is diagonal with diagonal entries $1 - e^{i\,2\,(\theta_{N+j} - \theta_j)}$, $\forall j \in \{1, 2, \ldots, J-N\}$, by virtue of Theorem 1, it can be stated that, when $N < J \leq 2\,N$, the augmented matrix $\mathbf{H}$ is full-column rank iff

$$\theta_{N+j} - \theta_j \neq h\,\pi, \;\; \forall j \in \{1, 2, \ldots, J-N\} \text{ and } h \in \mathbb{Z}\,. \quad (30)$$

As an immediate implication of (30), it is worth pointing out that, if no precoding is performed at the transmitter, i.e., $\theta_1 = \theta_2 = \cdots = \theta_J$, and common WH spreading codes are employed, the WL-MOE receiver is unable to achieve perfect MAI suppression in overloaded systems, even in the absence of noise. Henceforth, in order to allow WL-MUD to successfully work in an overloaded downlink, while employing WH spreading sequences, incorporation of precoding phases is crucial. This is the reason that motivated us to introduce the phases $\theta_1, \theta_2, \ldots, \theta_J$ in (1). It is worthwhile to observe that condition (30) does not uniquely specify the precoding phases and, thus, different choices can be pursued. To corroborate the previous considerations, we provide a numerical example.

Example 1: Consider a DS-CDMA downlink with $\alpha_1 = \alpha_2 = \cdots = \alpha_J = 1$ and processing gain $N = 16$, and without loss of generality, assume that the desired user is the first one (i.e., $j = 1$). The SNR, which is defined as $1/\sigma_v^2$, is set to 15 dB, and the signatures are generated according to (24). The system uses unit-norm WH vector codes and operates over a channel of order $L_g = 5$, whose taps $g(0), g(1), \ldots, g(5)$ are modeled as i.i.d. complex proper zero-mean Gaussian random variables, normalized so that $\|\boldsymbol{\psi}_j\|^2 = 1$, $\forall j \in \{1, 2, \ldots, J\}$. Fig. 2 reports the ideal SINR performance of the WL-MOE receiver as a function of the number of users J, ranging from an underloaded ($1 < J \leq N$) system to an overloaded ($N < J \leq 2\,N$) one. Specifically, we report $\text{SINR}_{1,\text{WL-MOE}}$ [see (20)] in two different situations: in the former one, there is no precoding at the transmitter, i.e., $\theta_1 = \theta_2 = \cdots = \theta_J = 0$ (referred to as "without precoding"); in the latter one, we use a precoding strategy fulfilling (30), by setting $\theta_1 = \theta_2 = \cdots = \theta_N = 0$ and $\theta_{N+1} = \theta_{N+2} = \cdots = \theta_{2N} = \pi/4$ (referred to as "with precoding"). The results of Fig. 2 are obtained by carrying out 10^4 independent Monte Carlo trials, with each run using only a different channel realization. It can be observed that, if WH spreading sequences are employed and condition (30) is not accounted for, the WL-MOE receiver does not work at all, when the system becomes overloaded. In contrast, the proposed precoding strategy allows the WL-MOE receiver to achieve a satisfactory performance even when $N < J \leq 2\,N$.

[10]In the uplink scenario, the full-column rank property of $\mathbf{H}$ and, thus, the performance of the WL-MOE receiver, depends not only on the precoding phases, but also on the channel impulse responses of all the active users.

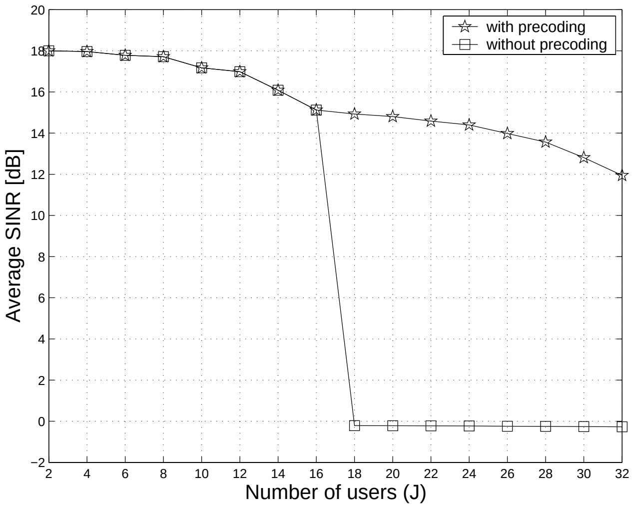

Fig. 2. Average SINR values of the WL-MOE receiver versus J for different precoding techniques (SNR = 15 dB).

V. Finite-sample performances of the L-MOE and WL-MOE receivers

In this section, two different data-estimated versions of the L-MOE and WL-MOE receivers are introduced, i.e., the WL receiver employing sample-matrix inversion (WL-SMI) and the WL receiver employing subspace decomposition (WL-SUB), and their finite-sample performance are evaluated by adopting a first-order perturbative approach [31], [32].

Starting from K samples of the received vector $\mathbf{r}(k)$, the WL-SMI receiver is obtained by replacing $\mathbf{R}_{\mathbf{zz}}$ in (18) with its sample estimate

$$\widehat{\mathbf{R}}_{\mathbf{zz}} = \frac{1}{K} \sum_{k=1}^{K} \mathbf{z}(k)\,\mathbf{z}^H(k)\,, \quad (31)$$

thus obtaining

$$\mathbf{f}_{j,\text{WL-SMI}} \triangleq (\mathbf{h}_j^H \widehat{\mathbf{R}}_{\mathbf{zz}}^{-1} \mathbf{h}_j)^{-1} \, \widehat{\mathbf{R}}_{\mathbf{zz}}^{-1} \, \mathbf{h}_j\,. \quad (32)$$

Note that, in the sequel, we assume that the desired channel impulse response (and thus $\mathbf{h}_j$) is exactly known at the receiver. The WL-SUB receiver resorts to the EVD of $\mathbf{R}_{\mathbf{zz}}$ to mitigate the performance degradation due to finite-sample-size effects. To this end, it is required[11] that the

[11]As a matter of fact, this assumption is not required for the WL-SMI receiver and it is necessary only for the WL-SUB one. However, since the WL-MOE receiver is not able to ensure perfect MAI suppression, for each user, when $\mathbf{H}$ is rank-deficient, we maintain the assumption $\text{rank}(\mathbf{H}) = J$ for both the two data-estimated WL receivers.

augmented matrix $\mathbf{H}$ is full-column rank (an issue that has been discussed in Section IV), which necessarily requires that $J \leq 2N$. Under this assumption, accounting for (12) and recalling that $\mathbf{R_{dd}} = \sigma_v^2 \mathbf{I}_{2N}$, the EVD of $\mathbf{R_{zz}}$ is given by $\mathbf{R_{zz}} = \mathbf{U}_s \boldsymbol{\Lambda}_s \mathbf{U}_s^H + \sigma_v^2 \mathbf{U}_n \mathbf{U}_n^H$, where $\mathbf{U}_s \in \mathbb{C}^{2N\times J}$ collects the eigenvectors associated with the J largest (signal- and noise-dependent) eigenvalues $\lambda_1, \lambda_2, \ldots, \lambda_J$ of $\mathbf{R_{zz}}$ (arranged in decreasing order), whose columns span the *signal subspace*, i.e., the column space $\mathcal{R}(\mathbf{H})$ of $\mathbf{H}$, while $\mathbf{U}_n \in \mathbb{C}^{2N\times(2N-J)}$ collects the eigenvectors associated with the eigenvalue σ_v^2, whose columns span the *noise subspace*, i.e., the orthogonal complement $\mathcal{R}^\perp(\mathbf{H})$ in $\mathbb{C}^{2N}$ of the signal subspace and, finally, $\boldsymbol{\Lambda}_s \triangleq \text{diag}(\lambda_1, \lambda_2, \ldots, \lambda_J)$. By substituting the EVD of $\mathbf{R_{zz}}$ in (18) and exploiting the orthogonality between signal and noise subspaces, one obtains

$$\mathbf{f}_{j,\text{WL-MOE}} = (\mathbf{h}_j^H \mathbf{U}_s \boldsymbol{\Lambda}_s^{-1} \mathbf{U}_s^H \mathbf{h}_j)^{-1} \mathbf{U}_s \boldsymbol{\Lambda}_s^{-1} \mathbf{U}_s^H \mathbf{h}_j . \quad (33)$$

Since in practice the EVD is performed on $\widehat{\mathbf{R}}_{\mathbf{zz}}$ given by (31), by denoting the sample matrices corresponding to $\mathbf{U}_s$ and $\boldsymbol{\Lambda}_s$ with $\widehat{\mathbf{U}}_s$ and $\widehat{\boldsymbol{\Lambda}}_s$, respectively, we have:

$$\mathbf{f}_{j,\text{WL-SUB}} \triangleq (\mathbf{h}_j^H \widehat{\mathbf{U}}_s \widehat{\boldsymbol{\Lambda}}_s^{-1} \widehat{\mathbf{U}}_s^H \mathbf{h}_j)^{-1} \widehat{\mathbf{U}}_s \widehat{\boldsymbol{\Lambda}}_s^{-1} \widehat{\mathbf{U}}_s^H \mathbf{h}_j . \quad (34)$$

It is worth noting that the weight vector $\mathbf{f}_{j,\text{WL-SUB}}$ is not equal to $\mathbf{f}_{j,\text{WL-SMI}}$, since $\widehat{\mathbf{U}}_n^H \mathbf{h}_j \neq \mathbf{0}_{2N-J}$ due to the finite-sample-size effects. This implies that the two receivers WL-SMI and WL-SUB might exhibit different SINR performances. To carry out the performance analysis for WL-SMI and WL-SUB in an unified framework, let us denote with $\widehat{\mathbf{f}}_j$ *any* data-estimated WL-MOE receiver, i.e, $\widehat{\mathbf{f}}_j = \mathbf{f}_{j,\text{WL-SMI}}$ or $\widehat{\mathbf{f}}_j = \mathbf{f}_{j,\text{WL-SUB}}$, and set $\mathbf{f}_j = \mathbf{f}_{j,\text{WL-MOE}}$ for simplicity, where $\mathbf{f}_{j,\text{WL-MOE}}$ is given by (18) or (33). Adopting a perturbation perspective, the vector $\widehat{\mathbf{f}}_j$ can be expressed as

$$\widehat{\mathbf{f}}_j = \mathbf{f}_j + \boldsymbol{\delta}\mathbf{f}_j , \quad (35)$$

where $\boldsymbol{\delta}\mathbf{f}_j$ is a *small* (i.e., $\|\boldsymbol{\delta}\mathbf{f}_j\| \ll 1$) zero-mean perturbation term. Since any data-estimated version of the WL-MOE receiver must satisfy the constraint $\widehat{\mathbf{f}}_j^H \mathbf{h}_j = 1$, it results that $\boldsymbol{\delta}\mathbf{f}_j^H \mathbf{h}_j = 0$, thus the SINR (15) for the data-estimated receivers can be written as

$$\text{SINR}(\widehat{\mathbf{f}}_j) = \frac{1}{\text{E}_{\widehat{\mathbf{f}}_j,\mathbf{q}_j}\left\{\text{Re}^2[\widehat{\mathbf{f}}_j^H \mathbf{q}_j(k)]\right\}} , \quad (36)$$

where the symbol $\text{E}_{\widehat{\mathbf{f}}_j,\mathbf{q}_j}[\cdot]$ denotes *joint* average w.r.t to $\widehat{\mathbf{f}}_j$ and $\mathbf{q}_j(k)$ of the quantity in brackets. A simplifying and reasonable assumption [33] is that $\widehat{\mathbf{f}}_j$ is independent from $\mathbf{q}_j(k)$. In this case, by accounting for the CS property of $\widehat{\mathbf{f}}_j$, substituting (35) into (36), performing the average w.r.t to $\mathbf{q}_j(k)$, and recalling that, due to assumptions **(a1)** and **(a2)**, the vector $\mathbf{q}_j(k)$ is zero-mean, one has:

$$\text{SINR}(\widehat{\mathbf{f}}_j) = \frac{1}{\mathbf{f}_j^H \mathbf{R}_{\mathbf{q}_j\mathbf{q}_j} \mathbf{f}_j + \text{E}_{\boldsymbol{\delta}\mathbf{f}_j}[\boldsymbol{\delta}\mathbf{f}_j^H \mathbf{R}_{\mathbf{q}_j\mathbf{q}_j} \boldsymbol{\delta}\mathbf{f}_j]} , \quad (37)$$

where only the average w.r.t to $\boldsymbol{\delta}\mathbf{f}_j$ must be evaluated. To perform this calculation, we need explicit expressions for the perturbation $\boldsymbol{\delta}\mathbf{f}_j$ of the WL-SMI and WL-SUB receivers, which are provided by the following Lemma.

Lemma 2: Assume that $\mathbf{H}$ is full-column rank and let $\widehat{\mathbf{R}}_{\mathbf{zz}}$ be estimated by (31). The *first-order* perturbation term of the WL-SMI and WL-SUB receivers can be expressed as

$$\boldsymbol{\delta}\mathbf{f}_j = -\boldsymbol{\Gamma}_{j,\text{WL}} \, \widehat{\mathbf{r}}_{\mathbf{q}_j b_j} , \quad (38)$$

where $\widehat{\mathbf{r}}_{\mathbf{q}_j b_j} \triangleq \frac{1}{K}\sum_{k=0}^{K-1} \mathbf{q}_j(k)\, b_j(k)$ is the sample estimate of the cross-correlation between the disturbance vector $\mathbf{q}_j(k)$ and the desired symbol $b_j(k)$, and

$$\boldsymbol{\Gamma}_{j,\text{WL}} = \begin{cases} \mathbf{P}_{j,\text{WL}} \mathbf{R}_{\mathbf{q}_j\mathbf{q}_j}^{-1} & \text{(WL-SMI)} \\ \mathbf{P}_{j,\text{WL}} \mathbf{R}_{\mathbf{q}_j\mathbf{q}_j}^{-1} - \gamma_{j,\text{WL}} \mathbf{U}_n \mathbf{U}_n^H & \text{(WL-SUB)} \end{cases} \quad (39)$$

with $\mathbf{P}_{j,\text{WL}} \triangleq \mathbf{I}_{2N} - (\mathbf{h}_j^H \mathbf{R}_{\mathbf{q}_j\mathbf{q}_j}^{-1} \mathbf{h}_j)^{-1} \mathbf{R}_{\mathbf{q}_j\mathbf{q}_j}^{-1} \mathbf{h}_j \mathbf{h}_j^H \in \mathbb{C}^{N\times N}$ denoting an oblique projection matrix [33], and $\gamma_{j,\text{WL}} \triangleq \sigma_v^{-2} + (\mathbf{h}_j^H \mathbf{R}_{\mathbf{zz}}^{-1} \mathbf{h}_j)^{-1} \mathbf{h}_j^H \mathbf{U}_s \boldsymbol{\Omega}_{\text{WL}}^{-1} \mathbf{U}_s^H \mathbf{R}_{\mathbf{zz}}^{-1} \mathbf{h}_j$, where $\boldsymbol{\Omega}_{\text{WL}} \triangleq \boldsymbol{\Lambda}_{\mathbf{s}} - \sigma_v^2 \mathbf{I}_J \in \mathbb{R}^{J\times J}$.

Proof: See Appendix D. ■

It should be observed that Lemma 2 provides a compact characterization of the perturbation terms, obtained under the simplifying assumption [33] that the predominant error in estimating $\mathbf{R_{zz}}$ is due to $\widehat{\mathbf{r}}_{\mathbf{q}_j b_j}$ (see Appendix D for details). This approximation will allows us to obtain simple yet accurate results, which will be validated in Section VI. Accounting for Lemma 2, the average in (37) can be expressed as (we drop the subscript $\boldsymbol{\delta}\mathbf{f}_j$ in $\text{E}_{\boldsymbol{\delta}\mathbf{f}_j}[\cdot]$ for notational simplicity)

$$\begin{aligned} \text{E}[\boldsymbol{\delta}\mathbf{f}_j^H \mathbf{R}_{\mathbf{q}_j\mathbf{q}_j} \boldsymbol{\delta}\mathbf{f}_j] &= \text{E}[\widehat{\mathbf{r}}_{\mathbf{q}_j b_j}^H \boldsymbol{\Gamma}_{j,\text{WL}}^H \mathbf{R}_{\mathbf{q}_j\mathbf{q}_j} \boldsymbol{\Gamma}_{j,\text{WL}} \widehat{\mathbf{r}}_{\mathbf{q}_j b_j}] \\ &= \text{trace}\{\boldsymbol{\Gamma}_{j,\text{WL}}^H \mathbf{R}_{\mathbf{q}_j\mathbf{q}_j} \boldsymbol{\Gamma}_{j,\text{WL}} \text{E}[\widehat{\mathbf{r}}_{\mathbf{q}_j b_j} \widehat{\mathbf{r}}_{\mathbf{q}_j b_j}^H]\} , \end{aligned} \quad (40)$$

where, by accounting for assumptions **(a1)** and **(a2)**, one has:

$$\begin{aligned} \text{E}[\widehat{\mathbf{r}}_{\mathbf{q}_j b_j} \widehat{\mathbf{r}}_{\mathbf{q}_j b_j}^H] &= \frac{1}{K^2} \sum_{k,h=1}^{K} \text{E}[\mathbf{q}_j(k)\, b_j(k)\, b_j(h)\, \mathbf{q}_j^H(h)] \\ &= \frac{1}{K^2} \sum_{k,h=1}^{K} \text{E}[\mathbf{q}_j(k)\, \mathbf{q}_j^H(h)]\, \text{E}[b_j(k)\, b_j(h)] \\ &= \frac{1}{K^2} \sum_{k,h=1}^{K} \text{E}[\mathbf{q}_j(k)\, \mathbf{q}_j^H(h)]\, \delta_{k-h} \\ &= \frac{1}{K^2} \sum_{k=1}^{K} \text{E}[\mathbf{q}_j(k)\, \mathbf{q}^H(k)] = \frac{1}{K} \mathbf{R}_{\mathbf{q}_j\mathbf{q}_j} . \end{aligned} \quad (41)$$

By substituting (41) in (40), the result back in (37), and recalling that $\mathbf{f}_j^H \mathbf{R}_{\mathbf{q}_j\mathbf{q}_j} \mathbf{f}_j = \text{SINR}_{j,\text{WL-MOE}}^{-1}$, where $\text{SINR}_{j,\text{WL-MOE}}$ is given by (20), we get

$$\text{SINR}(\widehat{\mathbf{f}}_j) = \frac{\text{SINR}_{j,\text{WL-MOE}}}{1 + \frac{\text{trace}(\boldsymbol{\Gamma}_{j,\text{WL}}^H \mathbf{R}_{\mathbf{q}_j\mathbf{q}_j} \boldsymbol{\Gamma}_{j,\text{WL}} \mathbf{R}_{\mathbf{q}_j\mathbf{q}_j})}{K} \text{SINR}_{j,\text{WL-MOE}}} . \quad (42)$$

The final result is obtained by evaluating the trace$(\cdot)$ term in (42), on the basis of the $\boldsymbol{\Gamma}_{j,\text{WL}}$ expressions given in Lemma 2. To do this, it is convenient to consider the SMI and SUB cases separately. With reference to the WL-SMI receiver, since

$\mathbf{\Gamma}_{j,\text{WL}} = \mathbf{P}_{j,\text{WL}}\,\mathbf{R}^{-1}_{\mathbf{q}_j\mathbf{q}_j}$, by using the properties of the trace operator, after some algebraic manipulations, one obtains:

$$\text{trace}(\mathbf{\Gamma}^H_{j,\text{WL}}\mathbf{R}_{\mathbf{q}_j\mathbf{q}_j}\,\mathbf{\Gamma}_{j,\text{WL}}\,\mathbf{R}_{\mathbf{q}_j\mathbf{q}_j}) = \frac{\text{trace}(\mathbf{P}_{j,\text{WL}}\,\mathbf{P}^H_{j,\text{WL}})}{K} = \frac{2\,N-1}{K}\,, \tag{43}$$

which can be substituted in (42), thus leading to

$$\text{SINR}_{j,\text{WL-SMI}} \triangleq \text{SINR}(\mathbf{f}_{j,\text{WL-SMI}}) = \frac{\text{SINR}_{j,\text{WL-MOE}}}{1+\frac{2\,N-1}{K}\,\text{SINR}_{j,\text{WL-MOE}}}\,. \tag{44}$$

As regards the WL-SUB receiver, since $\mathbf{\Gamma}_{j,\text{WL}} = \mathbf{P}_{j,\text{WL}}\,\mathbf{R}^{-1}_{\mathbf{q}_j\mathbf{q}_j} - \gamma_{j,\text{WL}}\,\mathbf{U}_n\,\mathbf{U}^H_n$, by using again the properties of the trace operator and observing that $\mathbf{U}^H_n\,\mathbf{h}_j = \mathbf{0}_{2N-J}$, after some algebra, one has:

$$\begin{aligned}&\text{trace}(\mathbf{\Gamma}^H_{j,\text{WL}}\mathbf{R}_{\mathbf{q}_j\mathbf{q}_j}\,\mathbf{\Gamma}_{j,\text{WL}}\,\mathbf{R}_{\mathbf{q}_j\mathbf{q}_j}) = \\ &= 2\,N-1-(\gamma^*_{j,\text{WL}}\,\sigma^2_v+\gamma_{j,\text{WL}}\,\sigma^2_v-|\gamma_{j,\text{WL}}\,\sigma^2_v|^2)(2N-J) \\ &= (J-1)+(2\,N-J)\,|1-\gamma_{j,\text{WL}}\,\sigma^2_v|^2\,. \end{aligned}\tag{45}$$

After substituting (45) into (42), one gets:

$$\text{SINR}_{j,\text{WL-SUB}} \triangleq \text{SINR}(\mathbf{f}_{j,\text{WL-SUB}}) = \frac{\text{SINR}_{j,\text{WL-MOE}}}{1+\frac{(J-1)+(2\,N-J)\,|1-\gamma_{j,\text{WL}}\,\sigma^2_v|^2}{K}\,\text{SINR}_{j,\text{WL-MOE}}}\,. \tag{46}$$

The expression (46) for the WL-SUB receiver can be further simplified by observing that, for $\sigma^2_v \to 0$, one has $\gamma_{j,\text{WL}}\,\sigma^2_v \to 1$, hence the trace in (45) reduces to $J-1$. By accounting for this observation, for moderate-to-high values of the SNR, eq. (46) can be approximatively written as

$$\text{SINR}_{j,\text{WL-SUB}} = \frac{\text{SINR}_{j,\text{WL-MOE}}}{1+\frac{J-1}{K}\,\text{SINR}_{j,\text{WL-MOE}}}\,. \tag{47}$$

It is worth noting that, despite of the apparent similarity between (44)–(47) and the SINR formulas reported in [18, eqs. (14) and (25)], our results are not directly comparable with those of [18]. Indeed, the results of [18] report the SINR performances of the LMS-based adaptive implementation of the WL-MMSE and WL-MOE receivers only for $K \to +\infty$ (steady-state performances); in this latter case the performance penalty paid by the WL-MUD receivers with respect to their ideal counterparts is exclusively due to gradient-noise effects.

The finite-sample performance analysis of the L-MOE receivers is now in order. Specifically, the L-SMI receiver is given by

$$\mathbf{g}_{j,\text{L-SMI}} \triangleq (\boldsymbol{\phi}^H_j\widehat{\mathbf{R}}^{-1}_{\mathbf{rr}}\boldsymbol{\phi}_j)^{-1}\,\widehat{\mathbf{R}}^{-1}_{\mathbf{rr}}\,\boldsymbol{\phi}_j \tag{48}$$

and is obtained by replacing $\mathbf{R}_{\mathbf{rr}}$ in (9) with its sample estimate

$$\widehat{\mathbf{R}}_{\mathbf{rr}} = \frac{1}{K}\sum_{k=1}^{K}\mathbf{r}(k)\,\mathbf{r}^H(k)\,. \tag{49}$$

Instead, the L-SUB receiver is defined as

$$\mathbf{g}_{j,\text{L-SUB}} \triangleq (\boldsymbol{\phi}^H_j\,\widehat{\mathbf{V}}_s\,\widehat{\mathbf{\Sigma}}^{-1}_s\,\widehat{\mathbf{V}}^H_s\,\boldsymbol{\phi}_j)^{-1}\,\widehat{\mathbf{V}}_s\,\widehat{\mathbf{\Sigma}}^{-1}_s\,\widehat{\mathbf{V}}^H_s\,\boldsymbol{\phi}_j\,, \tag{50}$$

where the columns of $\widehat{\mathbf{V}}_s \in \mathbb{C}^{N\times J}$ coincide with the eigenvectors corresponding to the J largest eigenvalues $\widehat{\mu}_1, \widehat{\mu}_2, \ldots, \widehat{\mu}_J$ (arranged in decreasing order) of the sample autocorrelation matrix $\widehat{\mathbf{R}}_{\mathbf{rr}}$, and $\widehat{\mathbf{\Sigma}}_s \triangleq \text{diag}(\widehat{\mu}_1, \widehat{\mu}_2, \ldots, \widehat{\mu}_J) \in \mathbb{R}^{J\times J}$. In order to carry out the performance analysis of the L-SMI and L-SUB receivers, it should be stressed that, since the relevant SINR is the one after the Re[·] part, one cannot simply apply results available in the literature (e.g., [32]), since they refer to the SINR evaluated before the Re[·] part. However, to avoid to be overwhelmed by mathematical derivations, we will report only the final results and defer to Appendix E for their proofs. Under the assumption that the matrix $\mathbf{\Phi}$ is full-column rank (see Section IV for a brief discussion regarding this issue), which necessarily requires that $J \le N$, it turns out that, in the high-SNR regime, the output SINR (15) of the L-SMI and L-SUB receivers can be approximatively written as

$$\text{SINR}_{j,\text{L-SMI}} \triangleq \text{SINR}(\mathbf{g}_{j,\text{L-SMI}}) = \frac{\text{SINR}_{j,\text{L-MOE}}}{1+\frac{N+J-2}{2\,K}\,\text{SINR}_{j,\text{L-MOE}}}\,, \tag{51}$$

$$\text{SINR}_{j,\text{L-SUB}} \triangleq \text{SINR}(\mathbf{g}_{j,\text{L-SUB}}) = \frac{\text{SINR}_{j,\text{L-MOE}}}{1+\frac{J-1}{K}\,\text{SINR}_{j,\text{L-MOE}}}\,. \tag{52}$$

Equations (44), (47), (51) and (52) allow one to easily compare the finite-sample performances of WL-MOE and L-MOE receivers. By comparing (47) and (52) for the subspace receivers, since $\text{SINR}_{j,\text{WL-MOE}} \ge \text{SINR}_{j,\text{L-MOE}}$ by (22), it turns out that $\text{SINR}_{j,\text{WL-SUB}} \ge \text{SINR}_{j,\text{L-SUB}}$ for any value of K and for $J \le N$. A similar conclusion does not hold for the SMI receivers. Indeed, it can be easily proven that, for $J < N$ it results that $\text{SINR}_{j,\text{WL-SMI}} \ge \text{SINR}_{j,\text{L-SMI}}$ only for $K \ge K_{\text{min}}$, where

$$K_{\text{min}} \triangleq \frac{3\,N-J}{2\,(\text{SINR}^{-1}_{j,\text{L-MOE}} - \text{SINR}^{-1}_{j,\text{WL-MOE}})} > 0 \tag{53}$$

is a threshold sample-size. In other words, it can be inferred that, in underloaded scenarios, the WL-SMI receiver assures the expected performance advantage over the L-SMI one only if a sufficient number of samples are processed. This loss of performance is due to the increase of the dimension of the autocorrelation matrix to be estimated from N to $2\,N$, which entails a diminished estimation accuracy, requiring hence a larger number of data samples for achieving a satisfactory performance, without resorting to subspace concepts.

Another interesting conclusion that can be drawn from (44) through (52) is that all finite-sample receivers exhibit a SINR saturation effect, i.e., a bit-error-rate (BER) floor, for vanishingly small noise. Indeed, when $\sigma^2_v \to 0$ and $\mathbf{H}$ is full-column rank ($J \le 2\,N$), it has been shown in Subsection IV-A that $\text{SINR}_{j,\text{WL-MOE}}$ grows without bound. Thus, accounting for (44) and (47), we get:

$$\begin{aligned}\lim_{\sigma^2_v\to 0}\text{SINR}_{j,\text{WL-SMI}} &= \frac{K}{2\,N-1}\,, \\ \lim_{\sigma^2_v\to 0}\text{SINR}_{j,\text{WL-SUB}} &= \frac{K}{J-1}\,,\end{aligned}\tag{54}$$

which show that, in the high-SNR regime, the performance of the WL-SMI receiver does not depend on the number of

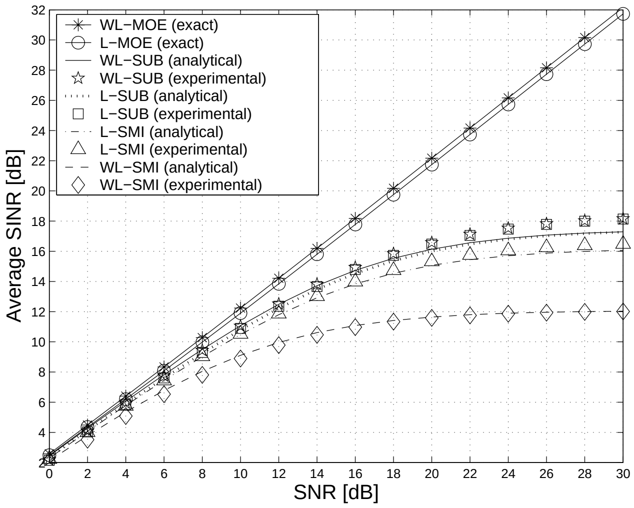

Fig. 3. Average SINR versus SNR ($J = 10$ users and $K = 500$ symbols).

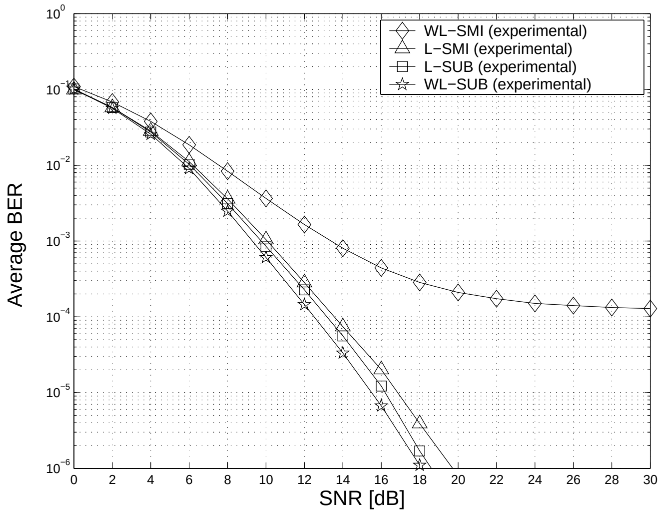

Fig. 4. Average BER versus SNR ($J = 10$ users and $K = 500$ symbols).

users J, whereas the asymptotic value of $\text{SINR}_{j,\text{WL-SUB}}$ is independent of the processing gain N. As regards the linear receivers, if $\sigma_v^2 \to 0$ and $\mathbf{\Phi}$ is full-column rank ($J \leq N$), then $\text{SINR}_{j,\text{L-MOE}} \to +\infty$ (see Subsection IV-A), which, accounting for (51) and (52), implies that

$$\lim_{\sigma_v^2 \to 0} \text{SINR}_{j,\text{L-SMI}} = \frac{2\,K}{N+J-2}\,, \qquad \lim_{\sigma_v^2 \to 0} \text{SINR}_{j,\text{L-SUB}} = \frac{K}{J-1}\,. \tag{55}$$

It can be seen that, while the WL-SUB and L-SUB receivers exhibit the same asymptotic SINR (for $J \leq N$), the L-SMI receiver for $J < N$ exhibits a better saturation SINR compared with the WL-SMI receiver, for any value of the sample size K. In conclusion, we can state that the advantages of WL receivers could be lost by employing simple estimation methods such as the SMI, whereas it is mandatory to resort to more sophisticated subspace-based methods based on EVD. It is worthwhile to note that in this latter case WL processing incurs an increased computational complexity compared with linear one, due to the increased dimension of the augmented correlation matrix, with respect to the conventional data autocorrelation matrix.

A. Numerical examples

Herein, we present the results of Monte Carlo computer simulations and compare them with the analytical results derived in Section V [see (44), (47), (51) and (52)]. Specifically, in all the examples, the same simulation setting considered in Example 1 is adopted (downlink scenario and $N = 16$), with $\theta_1 = \theta_2 = \cdots = \theta_N = 0$ and $\theta_{N+1} = \theta_{N+2} = \cdots = \theta_{2N} = \pi/4$ (we recall that this precoding strategy assures the full-column rank property of the augmented matrix $\mathbf{H}$ in overloaded scenarios). In addition, the symbol vector $\mathbf{b}(k)$ and the additive noise vector $\mathbf{v}(k)$ are generated according to assumptions **(a1)** and **(a2)**. For the sake of comparison, we consider both SMI- and SUB-based data-estimated versions of the L-MOE and WL-MOE receivers (wherein the channel impulse response is assumed to be exactly known), as well as their exact counterparts (wherein, besides the channel impulse response, perfect knowledge of the autocorrelation matrices $\mathbf{R_{rr}}$ and $\mathbf{R_{zz}}$ is assumed). Finally, as performance measure, in addition to the SINR given by (15) and averaged over 10^4 Monte Carlo runs, we resort to the average BER at the output of the considered receivers. More specifically, after estimating the receiver weight vectors on the basis of the given data record K, for each run (wherein, besides the channel impulse response, independent sets of noise and data sequences are randomly generated), an independent record of $K_{\text{ber}} = 10^3$ symbols is considered to evaluate the BER.

Example 2: In this example, we evaluate both the (average) SINR and BER performances of the considered receivers as a function of the SNR. The number of users is set equal to $J = 10$ (underloaded system) and the sample size is kept fixed to $K = 500$ symbols. Let us first consider the SINR performances, which are reported in Fig. 3. It can be seen that the analytical expressions (44), (47), (51) and (52) for the data-estimated linear and WL receivers agree very well with their corresponding simulation results, for all values of the SNR. In particular, in this underloaded scenario, while the L-SUB and WL-SUB receivers perform comparably, the WL-SMI receiver pays a significant performance loss with respect to the L-SMI one. Indeed, in the high-SNR region, the difference between the saturation values of $\text{SINR}_{1,\text{L-SMI}}$ and $\text{SINR}_{1,\text{WL-SMI}}$ is about 4 dB, which is in good agreement with (54) and (55). The unsatisfactory performance of the WL-SMI receiver is also apparent from Fig. 4, which depicts the BER curves of the data-estimated receivers under comparison. It is evident that the curves of the WL-SUB, L-SUB and L-SMI receivers go down very quickly as the SNR increases, thus assuring a huge performance gain with respect to the WL-SMI receiver, which instead exhibits a marked BER floor.

Example 3: Fig. 5 reports the SINR as a function of the number of users J. The SNR is set equal to 15 dB and $K = 500$ symbols are considered. Besides confirming the very good agreement between analytical and experimental

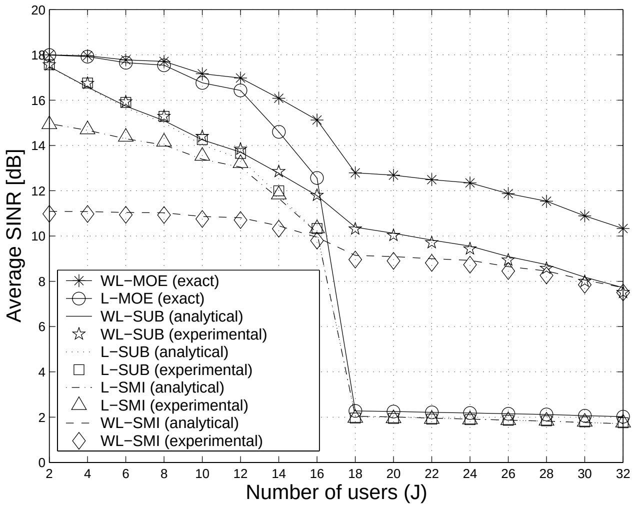

Fig. 5. Average SINR versus number of users ($K = 500$ symbols and SNR $= 15$ dB).

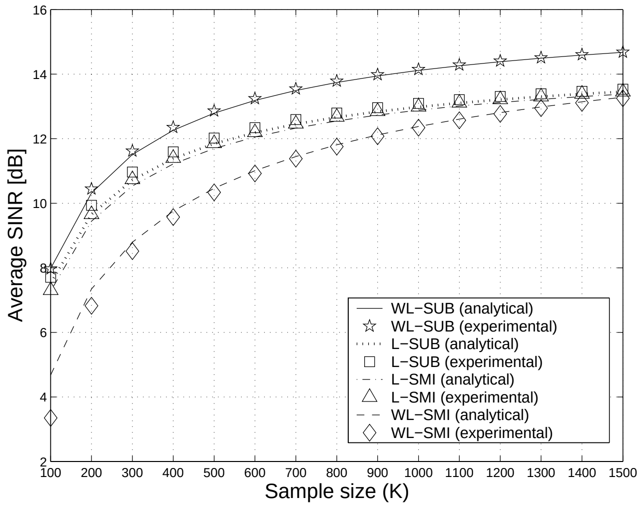

Fig. 6. Average SINR versus sample size K ($J = 14$ users and SNR $= 15$ dB).

results for all the data-estimated receivers, results of Fig. 5 show that the performances of all the linear receivers worsen very quickly when the system tends to be overloaded, i.e., J approaches $N = 16$. Beyond this value, the WL receivers assure a significant performance gain with respect to their corresponding linear counterparts. Loosely speaking, this indicates the ability of the WL-MOE receiver to accommodate twice the number of users of the L-MOE receiver.

Example 4: In this last experiment, we report the SINR performances of the considered data-estimated receivers as a function of the sample size K. The SNR is set equal to 15 dB and $J = 14$ users (underloaded system) are considered. It can be observed from Fig. 6 that the accuracy of the formulas (44), (47), (51) and (52) improves as K increases. Additionally, it is worth observing that the WL-SUB receiver outperforms the L-SUB one, for all the considered values of K. In contrast, the WL-SMI receiver performs worse than its corresponding linear counterpart, by approaching the curve of the L-SMI receiver only when the sample size K is as large as 1500 symbols, which agrees very well with the value $K_{\min} = 1686$ predicted by (53).

VI. CONCLUSIONS

We developed performance comparisons between ideal and data-estimated WL-MOE and L-MOE receivers. With reference to the ideal implementation, we investigated the relative performances of the WL-MOE and L-MOE receivers in the high-SNR regime. In this case, we provided a necessary and sufficient condition on the spreading codes, which allows the WL-MOE receiver to achieve perfect MAI suppression even in overloaded downlink configurations. As regards the data-estimated versions of the WL-MOE and L-MOE receivers, we derived easily interpretable formulas, which allow one to obtain clear insights about the effects of different parameters on performances. In a nutshell, compared with the L-MOE one, the performance of the WL-MOE receiver turns out to be more sensitive to finite-sample-size effects, and the performance gains predicted by the theory can be achieve in practice only by resorting to the more sophisticated subspace-based implementation. Finally, in this paper the channel impulse response was assumed to be exactly known at the receiving side and the precoding phases are not optimized. The assessment of the effects of channel-estimation errors and the optimization of the precoding phases are the topic of our current research and will be addressed in a forthcoming paper.

APPENDIX
PROOFS

A. Proof of Lemma 1

Any vector $\mathbf{f}_j \in \mathbb{C}^{2N}$ can be uniquely decomposed as $\mathbf{f}_j = \mathbf{f}_{j,\mathrm{s}} + \mathbf{f}_{j,\mathrm{a}}$, where we defined the *symmetric part* $\mathbf{f}_{j,\mathrm{s}} \in \mathcal{S} \triangleq \{\mathbf{f} = [\mathbf{f}_1^T, \mathbf{f}_2^T]^T \in \mathbb{C}^{2N} \,|\, \mathbf{f}_1 = \mathbf{f}_2^* \in \mathbb{C}^N\}$ and the *antisymmetric part* $\mathbf{f}_{j,\mathrm{a}} \in \mathcal{A} \triangleq \{\mathbf{f} = [\mathbf{f}_1^T, \mathbf{f}_2^T]^T \in \mathbb{C}^{2N} \,|\, \mathbf{f}_1 = -\mathbf{f}_2^* \in \mathbb{C}^N\}$. Since both $\mathbf{h}_j$ and $\mathbf{q}_j(k)$ in (14) are symmetric, i.e., they belong to $\mathcal{S}$, one has $\mathrm{Re}[\mathbf{f}_j^H\,\mathbf{h}_j] = \mathbf{f}_{j,\mathrm{s}}^H\,\mathbf{h}_j$ and $\mathrm{Re}[\mathbf{f}_j^H\,\mathbf{q}_j(k)] = \mathbf{f}_{j,\mathrm{s}}^H\,\mathbf{q}_j(k)$ in (15), that is, the SINR (15) is not affected by the antisymmetric part $\mathbf{f}_{j,\mathrm{a}}$. Hence, the weight vector $\mathbf{f}_{j,\text{max-SINR}}$ maximizing $\mathrm{SINR}(\mathbf{f}_j)$ given by (15) can equivalently be obtained by maximizing the following constrained cost function:

$$\mathrm{SINR}'(\mathbf{f}_j) \triangleq \frac{|\mathbf{f}_j^H\,\mathbf{h}_j|^2}{\mathrm{E}[|\mathbf{f}_j^H\,\mathbf{q}_j(k)|^2]} = \frac{|\mathbf{f}_j^H\mathbf{h}_j|^2}{\mathbf{f}_j^H\mathbf{R}_{\mathbf{q}_j\mathbf{q}_j}\mathbf{f}_j}\,, \quad \text{subject to } \mathbf{f}_j \in \mathcal{S}. \tag{56}$$

Note that in general $\mathrm{SINR}(\mathbf{f}_j) \neq \mathrm{SINR}'(\mathbf{f}_j)$, but they coincide for $\mathbf{f}_j \in \mathcal{S}$. The unconstrained maximization of $\mathrm{SINR}'(\mathbf{f}_j)$ leads [29] to the solution $\mathbf{f}'_{j,\text{max-SINR}} = \gamma_j\,\mathbf{R}_{\mathbf{q}_j\mathbf{q}_j}^{-1}\mathbf{h}_j$, with $\gamma_j \in \mathbb{C} - \{0\}$. At this point, we have to impose that $\mathbf{f}'_{j,\text{max-SINR}}$ satisfies the constraint $\mathbf{f}'_{j,\text{max-SINR}} \in \mathcal{S}$. To this respect, it can be verified that $\mathbf{R}_{\mathbf{q}_j\mathbf{q}_j}^{-1}\mathbf{h}_j \in \mathcal{S}$, hence, fulfillment of the constraint is ensured by imposing that γ_j be real, i.e., $\gamma_j = \gamma_j^*$. In conclusion, we can state that the general expression of the weight vector $\mathbf{f}_{j,\text{max-SINR}}$ maximizing $\mathrm{SINR}(\mathbf{f}_j)$ is given by

$\mathbf{f}_{j,\text{max-SINR}} = \xi_j \, \mathbf{R}_{\mathbf{q}_j \mathbf{q}_j}^{-1} \mathbf{h}_j$, with $\xi_j \triangleq \text{Re}[\gamma_j] \in \mathbb{R} - \{0\}$. The corresponding maximum value of $\text{SINR}(\mathbf{f}_j)$ turns out to be $\text{SINR}(\mathbf{f}_{j,\text{max-SINR}}) = \mathbf{h}_j^H \mathbf{R}_{\mathbf{q}_j \mathbf{q}_j}^{-1} \mathbf{h}_j$.

B. Relationships between $\overline{\text{SINR}}_{j,\text{max}}$, $\text{SINR}_{j,\text{L-MOE}}$ and $\text{SINR}_{j,\text{WL-MOE}}$ in the high-SNR regime

First of all, let us derive the expression of $\overline{\text{SINR}}_{j,\text{max}}$ [see (11)] in terms of σ_v^2. Under assumptions **(a1)–(a2)**, one has $\mathbf{R}_{\mathbf{p}_j \mathbf{p}_j} = \overline{\mathbf{\Phi}}_j \, \overline{\mathbf{\Phi}}_j^H + \sigma_v^2 \, \mathbf{I}_N$. Hence, by resorting to the EVD of $\overline{\mathbf{\Phi}}_j \, \overline{\mathbf{\Phi}}_j^H$, one obtains $\mathbf{R}_{\mathbf{p}_j \mathbf{p}_j} = \mathbf{V}_{j,s} \, \mathbf{\Sigma}_{j,s} \, \mathbf{V}_{j,s}^H + \sigma_v^2 \, \mathbf{I}_N$, where $\mathbf{V}_{j,s} \in \mathbb{C}^{N \times r_j}$ collects the eigenvectors associated with the r_j nonnull eigenvalues $\mu_{j,1}, \mu_{j,2}, \ldots, \mu_{j,r_j}$ of $\overline{\mathbf{\Phi}}_j \, \overline{\mathbf{\Phi}}_j^H$ (arranged in decreasing order), with $r_j \triangleq \text{rank}(\overline{\mathbf{\Phi}}_j) \leq \min\{N, J-1\}$ and $\mathbf{\Sigma}_{j,s} \triangleq \text{diag}(\mu_{j,1}, \mu_{j,2}, \ldots, \mu_{j,r_j}) \in \mathbb{R}^{r_j \times r_j}$. Relying on this decomposition and reasoning as in [34], the following series expansion of $\overline{\text{SINR}}_{j,\text{max}}$ holds:

$$
\begin{aligned}
\overline{\text{SINR}}_{j,\text{max}} &= \boldsymbol{\phi}_j^H \, \mathbf{R}_{\mathbf{p}_j \mathbf{p}_j}^{-1} \, \boldsymbol{\phi}_j \\
&= \frac{\boldsymbol{\phi}_j^H \mathbf{V}_{j,n} \, \mathbf{V}_{j,n}^H \, \boldsymbol{\phi}_j}{\sigma_v^2} + \boldsymbol{\phi}_j^H \mathbf{V}_{j,s} \, \mathbf{\Sigma}_{j,s}^{-1} \, \mathbf{V}_{j,s}^H \, \boldsymbol{\phi}_j + o(\sigma_v^2) \, , \quad (57)
\end{aligned}
$$

where $\mathbf{V}_{j,n} \in \mathbb{C}^{N \times (N - r_j)}$ collects the eigenvectors of $\overline{\mathbf{\Phi}}_j \, \overline{\mathbf{\Phi}}_j^H$ associated with its $N - r_j$ null eigenvalues. Eq. (57) shows that, as $\sigma_v^2 \to 0$, $\overline{\text{SINR}}_{j,\text{max}} \to +\infty$ if and only if (iff) $\boldsymbol{\phi}_j^H \mathbf{V}_{j,n} \, \mathbf{V}_{j,n}^H \, \boldsymbol{\phi}_j \neq 0$, which implies that $\boldsymbol{\phi}_j \notin \mathcal{N}(\mathbf{V}_{j,n}^H) \equiv \mathcal{R}(\overline{\mathbf{\Phi}}_j)$. It is noteworthy that this condition holds, $\forall j \in \{1, 2, \ldots, J\}$, iff the matrix $\mathbf{\Phi} \in \mathbb{C}^{N \times J}$ is full-column rank, i.e., $\text{rank}(\mathbf{\Phi}) = J$, which imposes that the number of users J must be smaller than or equal to the processing gain N (underloaded system). On the other hand, when $\boldsymbol{\phi}_j$ belongs to $\mathcal{R}(\overline{\mathbf{\Phi}}_j)$, it results that $\lim_{\sigma_v^2 \to 0} \overline{\text{SINR}}_{j,\text{max}} = \boldsymbol{\phi}_j^H \mathbf{V}_{j,s} \, \mathbf{\Sigma}_{j,s}^{-1} \, \mathbf{V}_{j,s}^H \, \boldsymbol{\phi}_j$, which evidences that, as $\sigma_v^2 \to 0$, $\overline{\text{SINR}}_{j,\text{max}}$ takes on a finite value.

At this point, we are able to establish the relationship existing between $\overline{\text{SINR}}_{j,\text{max}}$ and $\text{SINR}_{j,\text{L-MOE}}$ [see (11) and (21)], in the limiting case of vanishingly small noise. Preliminarily, we observe that, under assumptions **(a1)–(a2)**, one has $\mathbf{R}_{\mathbf{p}_j \mathbf{p}_j^*} = \overline{\mathbf{\Phi}}_j \, \overline{\mathbf{\Phi}}_j^T$. By substituting (9) in (21) and accounting for (11), after some algebraic manipulations, one obtains

$$
\begin{aligned}
\lim_{\sigma_v^2 \to 0} \frac{\text{SINR}_{j,\text{L-MOE}}}{\overline{\text{SINR}}_{j,\text{max}}} &= \frac{2}{1 + \lim\limits_{\sigma_v^2 \to 0} \frac{\text{Re}\left[\boldsymbol{\phi}_j^H \mathbf{R}_{\mathbf{p}_j \mathbf{p}_j}^{-1} \overline{\mathbf{\Phi}}_j \, (\overline{\mathbf{\Phi}}_j^H \mathbf{R}_{\mathbf{p}_j \mathbf{p}_j}^{-1})^* \, \boldsymbol{\phi}_j^*\right]}{\overline{\text{SINR}}_{j,\text{max}}}} \, . \quad (58)
\end{aligned}
$$

By resorting to the limit formula for the Moore-Penrose inverse [19], it can be seen that $\lim_{\sigma_v^2 \to 0} \mathbf{R}_{\mathbf{p}_j \mathbf{p}_j}^{-1} \overline{\mathbf{\Phi}}_j = (\overline{\mathbf{\Phi}}_j^H)^\dagger$ and $\lim_{\sigma_v^2 \to 0} \overline{\mathbf{\Phi}}_j^H \mathbf{R}_{\mathbf{p}_j \mathbf{p}_j}^{-1} = (\overline{\mathbf{\Phi}}_j)^\dagger$. Consequently, we get $\lim_{\sigma_v^2 \to 0} \text{Re}\big[\boldsymbol{\phi}_j^H \mathbf{R}_{\mathbf{p}_j \mathbf{p}_j}^{-1} \overline{\mathbf{\Phi}}_j \, (\overline{\mathbf{\Phi}}_j^H \mathbf{R}_{\mathbf{p}_j \mathbf{p}_j}^{-1})^* \, \boldsymbol{\phi}_j^*\big] = \text{Re}\big[\boldsymbol{\phi}_j^H \, (\overline{\mathbf{\Phi}}_j^H)^\dagger \, (\overline{\mathbf{\Phi}}_j^*)^\dagger \, \boldsymbol{\phi}_j^*\big]$, which can only assume finite values. Therefore, based on the previous discussion regarding the asymptotic expression of $\overline{\text{SINR}}_{j,\text{max}}$, by virtue of (57) and (58), we can conclude that, if $\mathbf{\Phi}$ is full-column rank, then

$$
\lim_{\sigma_v^2 \to 0} \frac{\text{SINR}_{j,\text{L-MOE}}}{\overline{\text{SINR}}_{j,\text{max}}} = 2 \, , \quad \forall j \in \{1, 2, \ldots, J\} \, , \quad (59)
$$

which additionally implies that, as $\sigma_v^2 \to 0$, $\text{SINR}_{j,\text{L-MOE}} \to +\infty$, $\forall j \in \{1, 2, \ldots, J\}$.

Let us now derive the expression of $\text{SINR}_{j,\text{WL-MOE}}$ [see (20)] in terms of σ_v^2. Under assumptions **(a1)–(a2)**, one has $\mathbf{R}_{\mathbf{q}_j \mathbf{q}_j} = \overline{\mathbf{H}}_j \, \overline{\mathbf{H}}_j^H + \sigma_v^2 \, \mathbf{I}_{2N}$. Reasoning as previously done for $\overline{\text{SINR}}_{j,\text{max}}$, we express $\text{SINR}_{j,\text{WL-MOE}}$ explicitly in terms of σ_v^2 as follows:

$$
\begin{aligned}
&\text{SINR}_{j,\text{WL-MOE}} = \mathbf{h}_j^H \, \mathbf{R}_{\mathbf{q}_j \mathbf{q}_j}^{-1} \, \mathbf{h}_j \\
&= \frac{\mathbf{h}_j^H \mathbf{U}_{j,n} \, \mathbf{U}_{j,n}^H \, \mathbf{h}_j}{\sigma_v^2} + \mathbf{h}_j^H \mathbf{U}_{j,s} \, \mathbf{\Lambda}_{j,s}^{-1} \, \mathbf{U}_{j,s}^H \, \mathbf{h}_j + o(\sigma_v^2) \, , \quad (60)
\end{aligned}
$$

where $\mathbf{U}_{j,s} \in \mathbb{C}^{2N \times \nu_j}$ collects the eigenvectors associated with the ν_j nonnull eigenvalues $\lambda_{j,1}, \lambda_{j,2}, \ldots, \lambda_{j,\nu_j}$ of $\overline{\mathbf{H}}_j \, \overline{\mathbf{H}}_j^H$ (arranged in decreasing order), with $\nu_j \triangleq \text{rank}(\overline{\mathbf{H}}_j) \leq \min\{2N, J-1\}$ and $\mathbf{\Lambda}_{j,s} \triangleq \text{diag}(\lambda_{j,1}, \lambda_{j,2}, \ldots, \lambda_{j,\nu_j}) \in \mathbb{R}^{\nu_j \times \nu_j}$, whereas $\mathbf{U}_{j,n} \in \mathbb{C}^{2N \times (2N - \nu_j)}$ collects the eigenvectors of $\overline{\mathbf{H}}_j \, \overline{\mathbf{H}}_j^H$ associated with its $2N - \nu_j$ null eigenvalues. It can be argued from (60) that, as $\sigma_v^2 \to 0$, $\text{SINR}_{j,\text{WL-MOE}} \to +\infty$ iff $\mathbf{h}_j^H \mathbf{U}_{j,n} \, \mathbf{U}_{j,n}^H \, \mathbf{h}_j \neq 0$, which implies that $\mathbf{h}_j \notin \mathcal{N}(\mathbf{U}_{j,n}^H) \equiv \mathcal{R}(\overline{\mathbf{H}}_j)$. On the other hand, when $\mathbf{h}_j$ belongs to $\mathcal{R}(\overline{\mathbf{H}}_j)$, it results that, as $\sigma_v^2 \to 0$, $\text{SINR}_{j,\text{WL-MOE}}$ takes on the finite value $\mathbf{h}_j^H \mathbf{U}_{j,s} \, \mathbf{\Lambda}_{j,s}^{-1} \, \mathbf{U}_{j,s}^H \, \mathbf{h}_j$. Therefore, since condition $\mathbf{h}_j \notin \mathcal{R}(\overline{\mathbf{H}}_j)$ holds, $\forall j \in \{1, 2, \ldots, J\}$, iff the augmented matrix $\mathbf{H} = [\mathbf{\Phi}^T, \mathbf{\Phi}^H]^T \in \mathbb{C}^{2N \times J}$ is full-column rank, we maintain that, in the absence of noise, the WL-MOE receiver is able to achieve perfect MAI suppression for *each* active user iff $\text{rank}(\mathbf{H}) = J$. The matrix $\mathbf{H}$ turns out to be full-column rank iff the null spaces of the matrices $\mathbf{\Phi}$ and $\mathbf{\Phi}^*$ intersect only trivially (see, e.g., [23]), that is, $\mathcal{N}(\mathbf{\Phi}) \cap \mathcal{N}(\mathbf{\Phi}^*) = \{\mathbf{0}_J\}$. If $\mathbf{\Phi}$ is full-column rank, which necessarily requires that $J \leq N$ (underloaded system), this condition is trivially satisfied and, hence, the augmented matrix $\mathbf{H}$ is full-column rank as well. However, the converse statement is not true, that is, $\mathbf{H}$ may be full-column rank even when $N < J \leq 2N$ (overloaded system). To point out a first consequence of this result, let us focus attention on the case when $N < J \leq 2N$. In this overloaded scenario, the matrix $\mathbf{\Phi}$ cannot be full-column rank and, thus, it results that, as $\sigma_v^2 \to 0$, $\text{SINR}_{j,\text{L-MOE}}$ takes on a finite value. In contrast, since $\mathbf{H}$ can still be full-column rank in an overloaded system, relying on the results provided before, we can infer that, if $\mathbf{H}$ is full-column rank, then

$$
\lim_{\sigma_v^2 \to 0} \frac{\text{SINR}_{j,\text{WL-MOE}}}{\text{SINR}_{j,\text{L-MOE}}} = +\infty \, , \quad (61)
$$

$\forall j \in \{1, 2, \ldots, J\}$, with $N < J \leq 2N$. Let us now consider an underloaded scenario ($J \leq N$) and assume that $\mathbf{\Phi}$ is full-column rank. Since in this case the matrix $\mathbf{H}$ is full-column rank, too, it follows that both $\text{SINR}_{j,\text{L-MOE}}$ and $\text{SINR}_{j,\text{WL-MOE}}$ diverge, in the limiting case of vanishingly small noise, and thus $\lim_{\sigma_v^2 \to 0} \frac{\text{SINR}_{j,\text{WL-MOE}}}{\text{SINR}_{j,\text{L-MOE}}}$ assumes an indeterminate form. To overcome this mathematical difficulty, we preliminary develop the relationship existing between $\text{SINR}_{j,\text{WL-MOE}}$ and $\overline{\text{SINR}}_{j,\text{max}}$

in the high-SNR regime, by resorting to the series expansions (57) and (60). So doing, we get:

$$\lim_{\sigma_v^2 \to 0} \frac{\text{SINR}_{j,\text{WL-MOE}}}{\overline{\text{SINR}}_{j,\max}} = \frac{\mathbf{h}_j^H \mathbf{U}_{j,n} \mathbf{U}_{j,n}^H \mathbf{h}_j}{\boldsymbol{\phi}_j^H \mathbf{V}_{j,n} \mathbf{V}_{j,n}^H \boldsymbol{\phi}_j} = \frac{\|\mathbf{U}_{j,n}^H \mathbf{h}_j\|^2}{\|\mathbf{V}_{j,n}^H \boldsymbol{\phi}_j\|^2} , \tag{62}$$

where, since both $\boldsymbol{\Phi}$ and $\mathbf{H}$ are full-column rank, it follows that $\|\mathbf{V}_{j,n}^H \boldsymbol{\phi}_j\| \neq 0$ and $\|\mathbf{U}_{j,n}^H \mathbf{h}_j\| \neq 0$, $\forall j \in \{1, 2, \ldots, J\}$. It is worth observing that $\mathbf{V}_{j,n} \mathbf{V}_{j,n}^H$ and $\mathbf{U}_{j,n} \mathbf{U}_{j,n}^H$ represent the orthogonal projections [19] onto the subspaces $\mathcal{R}^{\perp}(\overline{\boldsymbol{\Phi}}_j)$ and $\mathcal{R}^{\perp}(\overline{\mathbf{H}}_j)$, respectively, which can be equivalently expressed [19] as $\mathbf{V}_{j,n} \mathbf{V}_{j,n}^H = \mathbf{I}_N - \overline{\boldsymbol{\Phi}}_j (\overline{\boldsymbol{\Phi}}_j^H \overline{\boldsymbol{\Phi}}_j)^{-1} \overline{\boldsymbol{\Phi}}_j^H$ and $\mathbf{U}_{j,n} \mathbf{U}_{j,n}^H = \mathbf{I}_{2N} - \overline{\mathbf{H}}_j (\overline{\mathbf{H}}_j^H \overline{\mathbf{H}}_j)^{-1} \overline{\mathbf{H}}_j^H$. By substituting this two relations in (62), and remembering that $\overline{\mathbf{H}}_j = [\overline{\boldsymbol{\Phi}}_j^T, \overline{\boldsymbol{\Phi}}_j^H]^T$ and $\mathbf{h}_j = [\boldsymbol{\phi}_j^T, \boldsymbol{\phi}_j^H]^T$, after some algebraic manipulations, one has:

$$\lim_{\sigma_v^2 \to 0} \frac{\text{SINR}_{j,\text{WL-MOE}}}{\overline{\text{SINR}}_{j,\max}} = 2 \cdot \frac{\|\boldsymbol{\phi}_j\|^2 - \text{Re}[\boldsymbol{\phi}_j^H \overline{\boldsymbol{\Phi}}_j] \{\text{Re}[\overline{\boldsymbol{\Phi}}_j^H \overline{\boldsymbol{\Phi}}_j]\}^{-1} \text{Re}[\overline{\boldsymbol{\Phi}}_j^H \boldsymbol{\phi}_j]}{\|\boldsymbol{\phi}_j\|^2 - \boldsymbol{\phi}_j^H \overline{\boldsymbol{\Phi}}_j (\overline{\boldsymbol{\Phi}}_j^H \overline{\boldsymbol{\Phi}}_j)^{-1} \overline{\boldsymbol{\Phi}}_j^H \boldsymbol{\phi}_j} . \tag{63}$$

Therefore, if $\boldsymbol{\Phi}$ is full-column rank, accounting for (59) and (63), we can state that:

$$\begin{aligned} \lim_{\sigma_v^2 \to 0} \frac{\text{SINR}_{j,\text{WL-MOE}}}{\text{SINR}_{j,\text{L-MOE}}} &= \lim_{\sigma_v^2 \to 0} \frac{\text{SINR}_{j,\text{WL-MOE}}}{\overline{\text{SINR}}_{j,\max}} \cdot \lim_{\sigma_v^2 \to 0} \frac{\overline{\text{SINR}}_{j,\max}}{\text{SINR}_{j,\text{L-MOE}}} \\ &= \frac{\|\boldsymbol{\phi}_j\|^2 - \text{Re}[\boldsymbol{\phi}_j^H \overline{\boldsymbol{\Phi}}_j] \{\text{Re}[\overline{\boldsymbol{\Phi}}_j^H \overline{\boldsymbol{\Phi}}_j]\}^{-1} \text{Re}[\overline{\boldsymbol{\Phi}}_j^H \boldsymbol{\phi}_j]}{\|\boldsymbol{\phi}_j\|^2 - \boldsymbol{\phi}_j^H \overline{\boldsymbol{\Phi}}_j (\overline{\boldsymbol{\Phi}}_j^H \overline{\boldsymbol{\Phi}}_j)^{-1} \overline{\boldsymbol{\Phi}}_j^H \boldsymbol{\phi}_j} . \end{aligned} \tag{64}$$

C. Proof of Theorem 1

Accounting for (1) and (24), and exploiting the fact that $\boldsymbol{\Theta}^* \boldsymbol{\Theta} = \mathbf{I}_N$, one has:

$$\mathbf{H} = \begin{bmatrix} \mathbf{G} & \mathbf{O}_{N \times N} \\ \mathbf{O}_{N \times N} & \mathbf{G}^* \end{bmatrix} \begin{bmatrix} \mathbf{C} \\ \mathbf{C}^* (\boldsymbol{\Theta}^2)^* \end{bmatrix} \boldsymbol{\Theta} \mathbf{A} , \tag{65}$$

which, as a consequence of the nonsingularity of matrices $\mathbf{G}$, $\mathbf{A}$ and $\boldsymbol{\Theta}$, implies that rank$(\mathbf{H})$ = rank$([\mathbf{C}^T, (\mathbf{C}\,\boldsymbol{\Theta}^2)^H]^T)$. In its turn, the matrix $[\mathbf{C}^T, (\mathbf{C}\,\boldsymbol{\Theta}^2)^H]^T \in \mathbb{C}^{2N \times J}$ is full-column rank iff $\mathcal{N}(\mathbf{C}) \cap \mathcal{N}[\mathbf{C}^* (\boldsymbol{\Theta}^2)^*] = \{\mathbf{0}_J\}$. At this point, let us characterize the null spaces of $\mathbf{C}$ and $\mathbf{C}^* (\boldsymbol{\Theta}^2)^*$, when $N < J \leq 2N$. In this overloaded case, by assuming without loss of generality that the first N column $\mathbf{c}_1$, $\mathbf{c}_2, \ldots, \mathbf{c}_N$ of $\mathbf{C}$ are linearly independent, its remaining $J - N$ columns $\mathbf{c}_{N+1}$, $\mathbf{c}_{N+2}, \ldots, \mathbf{c}_J$ can be expressed as a linear combination of the first N ones, thus obtaining the following decomposition $\mathbf{C} = \mathbf{C}_{\text{left}} [\mathbf{I}_N, \boldsymbol{\Pi}]$, where $\mathbf{C}_{\text{left}} \triangleq [\mathbf{c}_1, \mathbf{c}_2, \ldots, \mathbf{c}_N] \in \mathbb{C}^{N \times N}$ is nonsingular and $\boldsymbol{\Pi} \in \mathbb{C}^{N \times (J-N)}$ is a tall matrix. Due to nonsingularity of $\mathbf{C}_{\text{left}}$, it follows that $\mathcal{N}(\mathbf{C}) = \mathcal{N}([\mathbf{I}_N, \boldsymbol{\Pi}])$. Hence, it can be verified that the general forms of a vector $\boldsymbol{\alpha}_1 \in \mathbb{C}^J$ belonging to $\mathcal{N}(\mathbf{C})$ and a vector $\boldsymbol{\alpha}_2 \in \mathbb{C}^J$ belonging to $\mathcal{N}[\mathbf{C}^* (\boldsymbol{\Theta}^2)^*]$ are given by

$$\boldsymbol{\alpha}_1 = \begin{bmatrix} -\boldsymbol{\Pi} \\ \mathbf{I}_{J-N} \end{bmatrix} \boldsymbol{\vartheta}_1 \quad \text{and} \quad \boldsymbol{\alpha}_2 = \boldsymbol{\Theta}^2 \begin{bmatrix} -\boldsymbol{\Pi}^* \\ \mathbf{I}_{J-N} \end{bmatrix} \boldsymbol{\vartheta}_2 , \tag{66}$$

with arbitrary $\boldsymbol{\vartheta}_1, \boldsymbol{\vartheta}_2 \in \mathbb{C}^{J-N}$. By virtue of (66), the matrix $\mathbf{H}$ is not full-column rank iff there exist at least two nonzero vectors $\boldsymbol{\vartheta}_1$ and $\boldsymbol{\vartheta}_2$ such that $\boldsymbol{\alpha}_1 = \boldsymbol{\alpha}_2$, which amounts to $\boldsymbol{\Pi}\,\boldsymbol{\vartheta}_1 = \boldsymbol{\Theta}_1^2\,\boldsymbol{\Pi}^* \boldsymbol{\vartheta}_2$ and $\boldsymbol{\vartheta}_1 = \boldsymbol{\Theta}_2^2\,\boldsymbol{\vartheta}_2$, with $\boldsymbol{\Theta}_1 \triangleq \text{diag}(e^{i\,\theta_1}, e^{i\,\theta_2}, \ldots, e^{i\,\theta_N}) \in \mathbb{C}^{N \times N}$ and $\boldsymbol{\Theta}_2 \triangleq \text{diag}(e^{i\,\theta_{N+1}}, e^{i\,\theta_{N+2}}, \ldots, e^{i\,\theta_J}) \in \mathbb{C}^{(J-N)\times(J-N)}$. By substituting the second relation in the first one and observing that $\boldsymbol{\Theta}_1^2$ is nonsingular, one obtains $[\boldsymbol{\Pi}^* - (\boldsymbol{\Theta}_1^2)^*\,\boldsymbol{\Pi}\,\boldsymbol{\Theta}_2^2]\,\boldsymbol{\vartheta}_2 = \mathbf{0}_N$, which shows that, if the matrix $\boldsymbol{\Pi}^* - (\boldsymbol{\Theta}_1^2)^*\,\boldsymbol{\Pi}\,\boldsymbol{\Theta}_2^2 \in \mathbb{C}^{N \times (J-N)}$ is full-column rank, then $\boldsymbol{\alpha}_1 = \boldsymbol{\alpha}_2$ is satisfied iff $\boldsymbol{\vartheta}_1 = \boldsymbol{\vartheta}_2 = \mathbf{0}_{J-N}$. This assures that rank$(\mathbf{H}) = J$, since it means that $\mathcal{N}(\mathbf{C}) \cap \mathcal{N}[\mathbf{C}^* (\boldsymbol{\Theta}^2)^*] = \{\mathbf{0}_J\}$.

D. Proof of Lemma 2

First, let us consider the SMI implementation of the WL-MOE receiver. By substituting (12) in (31), the sample autocorrelation matrix $\widehat{\mathbf{R}}_{\mathbf{zz}}$ of the augmented vector $\mathbf{z}(k)$ can be expressed as

$$\widehat{\mathbf{R}}_{\mathbf{zz}} = \mathbf{h}_j\,\mathbf{h}_j^H + \mathbf{h}_j\,\widehat{\mathbf{r}}_{\mathbf{q}_j b_j}^H + \widehat{\mathbf{r}}_{\mathbf{q}_j b_j}\mathbf{h}_j^H + \widehat{\mathbf{R}}_{\mathbf{q}_j \mathbf{q}_j} , \tag{67}$$

where $\widehat{\mathbf{r}}_{\mathbf{q}_j b_j} \triangleq \frac{1}{K}\sum_{k=0}^{K-1} \mathbf{q}_j(k)\, b_j(k)$ and $\widehat{\mathbf{R}}_{\mathbf{q}_j \mathbf{q}_j} \triangleq \frac{1}{K}\sum_{k=0}^{K-1} \mathbf{q}_j(k)\,\mathbf{q}_j^H(k)$ represent sample estimates of the cross-correlation between the disturbance vector $\mathbf{q}_j(k)$ and the desired symbol $b_j(k)$, and the autocorrelation matrix of $\mathbf{q}_j(k)$, respectively. It is shown in [33] that, for moderate-to-high values of the sample size, i.e., $K \geq 6\,N$, the predominant cause of SINR degradation is represented by $\widehat{\mathbf{r}}_{\mathbf{q}_j b_j}$ and, thus, replacing $\widehat{\mathbf{R}}_{\mathbf{q}_j \mathbf{q}_j}$ with $\mathbf{R}_{\mathbf{q}_j \mathbf{q}_j}$ in (67) has a very marginal effect on the SINR. Therefore, remembering that $\mathbf{R}_{\mathbf{zz}} = \mathbf{h}_j \mathbf{h}_j^H + \mathbf{R}_{\mathbf{q}_j \mathbf{q}_j}$, eq. (67) can be rewritten as $\widehat{\mathbf{R}}_{\mathbf{zz}} = \mathbf{R}_{\mathbf{zz}} + \mathbf{h}_j\,\widehat{\mathbf{r}}_{\mathbf{q}_j b_j}^H + \widehat{\mathbf{r}}_{\mathbf{q}_j b_j}\mathbf{h}_j^H$. Its inverse admits [19] the following first-order approximation $\widehat{\mathbf{R}}_{\mathbf{zz}}^{-1} \approx \mathbf{R}_{\mathbf{zz}}^{-1} - \mathbf{R}_{\mathbf{zz}}^{-1}(\mathbf{h}_j\,\widehat{\mathbf{r}}_{\mathbf{q}_j b_j}^H + \widehat{\mathbf{r}}_{\mathbf{q}_j b_j}\mathbf{h}_j^H)\,\mathbf{R}_{\mathbf{zz}}^{-1}$, which can be substituted in (32), thus obtaining

$$\begin{aligned} \mathbf{f}_{j,\text{WL-SMI}} &\approx \mathbf{f}_{j,\text{WL-MOE}} \underbrace{-\mathbf{P}_{j,\text{WL}}\,\mathbf{R}_{\mathbf{zz}}^{-1}\,\widehat{\mathbf{r}}_{\mathbf{q}_j b_j}}_{\delta\mathbf{f}_{j,\text{WL-SMI}}} \\ &= \mathbf{f}_{j,\text{WL-MOE}} + \boldsymbol{\delta}\mathbf{f}_{j,\text{WL-SMI}} , \end{aligned} \tag{68}$$

with $\mathbf{P}_{j,\text{WL}} \triangleq \mathbf{I}_{2N} - (\mathbf{h}_j^H\,\mathbf{R}_{\mathbf{zz}}^{-1}\,\mathbf{h}_j)^{-1}\,\mathbf{R}_{\mathbf{zz}}^{-1}\,\mathbf{h}_j\,\mathbf{h}_j^H = \mathbf{I}_{2N} - (\mathbf{h}_j^H\,\mathbf{R}_{\mathbf{q}_j \mathbf{q}_j}^{-1}\,\mathbf{h}_j)^{-1}\,\mathbf{R}_{\mathbf{q}_j \mathbf{q}_j}^{-1}\,\mathbf{h}_j\,\mathbf{h}_j^H \in \mathbb{C}^{N \times N}$, where here and in the sequel the symbol $\approx$ denotes *first-order equality*, i.e., we neglect all the summands that tend to zero, as the sample size K approaches infinity, faster than the norm of the corresponding perturbation term. It is easily verified that $\mathbf{P}_{j,\text{WL}}\,\mathbf{R}_{\mathbf{zz}}^{-1} = \mathbf{P}_{j,\text{WL}}\,\mathbf{R}_{\mathbf{q}_j \mathbf{q}_j}^{-1}$.

At this point, we focus attention on the subspace implementation of the WL-MOE receiver. Preliminary, we observe that the EVD of $\widehat{\mathbf{R}}_{\mathbf{zz}}$ is given by

$$\widehat{\mathbf{R}}_{\mathbf{zz}} = \widehat{\mathbf{U}}_s\,\widehat{\boldsymbol{\Lambda}}_s\,\widehat{\mathbf{U}}_s^H + \widehat{\mathbf{U}}_n\,\widehat{\boldsymbol{\Lambda}}_n\,\widehat{\mathbf{U}}_n^H , \tag{69}$$

where $\widehat{\mathbf{U}}_s$, $\widehat{\boldsymbol{\Lambda}}_s$, $\widehat{\mathbf{U}}_n$ and $\widehat{\boldsymbol{\Lambda}}_n$ are sample estimates of $\mathbf{U}_s$, $\boldsymbol{\Lambda}_s$, $\mathbf{U}_n$ and $\sigma_v^2\,\mathbf{I}_N$, respectively. When $\mathbf{R}_{\mathbf{zz}}$ is estimated from the received data as in (31), for a sufficiently large sample size K, the estimate can be decomposed as $\widehat{\mathbf{R}}_{\mathbf{zz}} = \mathbf{R}_{\mathbf{zz}} + \boldsymbol{\delta}\mathbf{R}_{\mathbf{zz}}$, where $\boldsymbol{\delta}\mathbf{R}_{\mathbf{zz}}$ is a *small* additive perturbation (in the Frobenius norm sense). Consequently, the matrices $\widehat{\mathbf{U}}_s$ and $\widehat{\mathbf{\Lambda}}_s$ can be written [31], [32] as $\widehat{\mathbf{U}}_s = \mathbf{U}_s + \boldsymbol{\delta}\mathbf{U}_s$ and $\widehat{\mathbf{\Lambda}}_s = \mathbf{\Lambda}_s + \boldsymbol{\delta}\mathbf{\Lambda}_s$, where $\boldsymbol{\delta}\mathbf{U}_s$ and $\boldsymbol{\delta}\mathbf{\Lambda}_s$ represent the resulting perturbation in the estimated signal subspace, whose norm is of the order of $\|\boldsymbol{\delta}\mathbf{R}_{\mathbf{zz}}\|$. It results [31], [32] that $\boldsymbol{\delta}\mathbf{U}_s \approx \mathbf{U}_n \mathbf{U}_n^H \boldsymbol{\delta}\mathbf{R}_{\mathbf{zz}} \,\mathbf{\Omega}_{\text{WL}}^{-1}$, with $\mathbf{\Omega}_{\text{WL}} \triangleq \mathbf{\Lambda}_{\mathbf{s}} - \sigma_v^2 \mathbf{I}_J$, and $\boldsymbol{\delta}\mathbf{\Lambda}_s \approx \mathbf{U}_s^H \boldsymbol{\delta}\mathbf{R}_{\mathbf{zz}}\, \mathbf{U}_s$. By substituting the above expressions of $\widehat{\mathbf{U}}_s$ and $\widehat{\mathbf{\Lambda}}_s$ in (34), and remembering that $\mathbf{P}_{j,\text{WL}} \mathbf{R}_{\mathbf{zz}}^{-1} = \mathbf{P}_{j,\text{WL}} \mathbf{R}_{\mathbf{q}_j\mathbf{q}_j}^{-1}$, we get:

$$\begin{aligned}\mathbf{f}_{j,\text{WL-SUB}} &\approx \mathbf{f}_{j,\text{WL-MOE}} \\ &\underbrace{-\left(\mathbf{P}_{j,\text{WL}} \mathbf{R}_{\mathbf{q}_j\mathbf{q}_j}^{-1} - \gamma_{j,\text{WL}}\, \mathbf{U}_n \mathbf{U}_n^H\right) \widehat{\mathbf{r}}_{\mathbf{q}_j b_j}}_{\boldsymbol{\delta}\mathbf{f}_{j,\text{WL-SUB}}} \\ &= \mathbf{f}_{j,\text{WL-MOE}} + \boldsymbol{\delta}\mathbf{f}_{j,\text{WL-SUB}} , \end{aligned} \quad (70)$$

where $\gamma_{j,\text{WL}} \triangleq \sigma_v^{-2} + (\mathbf{h}_j^H \mathbf{R}_{\mathbf{zz}}^{-1} \mathbf{h}_j)^{-1} \mathbf{h}_j^H \mathbf{U}_s \mathbf{\Omega}_{\text{WL}}^{-1} \mathbf{U}_s^H \mathbf{R}_{\mathbf{zz}}^{-1} \mathbf{h}_j$.

E. Performance analysis of the L-SMI and L-SUB receivers

From a unified perspective, let us denote with $\widehat{\mathbf{g}}_j$ *any* data-estimated L-MOE receiver, i.e, $\widehat{\mathbf{g}}_j = \mathbf{g}_{j,\text{L-SMI}}$ or $\widehat{\mathbf{g}}_j = \mathbf{g}_{j,\text{L-SUB}}$, and set $\mathbf{g}_j = \mathbf{g}_{j,\text{L-MOE}}$ for simplicity. Adopting a perturbation approach, the vector $\widehat{\mathbf{g}}_j$ can be expressed as

$$\widehat{\mathbf{g}}_j = \mathbf{g}_j + \boldsymbol{\delta}\mathbf{g}_j , \quad (71)$$

where $\boldsymbol{\delta}\mathbf{g}_j$ is a *small* (in the Frobenius norm sense) zero-mean additive perturbation. Since any data-estimated version of the L-MOE receiver must satisfy the constraint $\widehat{\mathbf{g}}_j^H \boldsymbol{\phi}_j = 1$, it results that $\boldsymbol{\delta}\mathbf{g}_j^H \boldsymbol{\phi}_j = 0$. Thus, using the identity $\text{Re}^2[z] = \frac{1}{2}\{|z|^2 + \text{Re}[z^2]\}$, $\forall z \in \mathbb{C}$, the SINR (15) for data-estimated linear receivers becomes

$$\text{SINR}(\widehat{\mathbf{g}}_j) = \frac{2}{\text{E}_{\widehat{\mathbf{g}}_j,\mathbf{p}_j}\left\{|\widehat{\mathbf{g}}_j^H \mathbf{p}_j(k)|^2\right\} + \text{E}_{\widehat{\mathbf{g}}_j,\mathbf{p}_j}\left\{\text{Re}[(\widehat{\mathbf{g}}_j^H \mathbf{p}_j(k))^2]\right\}} . \quad (72)$$

Similarly to the WL case, we assume that $\widehat{\mathbf{g}}_j$ is independent from $\mathbf{p}_j(k)$. In this case, by substituting (71) into (72), performing the average w.r.t to $\mathbf{p}_j(k)$, and recalling that, due to assumptions **(a1)** and **(a2)**, the vector $\mathbf{p}_j(k)$ is zero-mean, one has

$$\begin{aligned}\text{SINR}(\widehat{\mathbf{g}}_j)^{-1} = \frac{1}{2}\Big\{ &\mathbf{g}_j^H \mathbf{R}_{\mathbf{p}_j\mathbf{p}_j} \mathbf{g}_j + \text{E}_{\boldsymbol{\delta}\mathbf{g}_j}[\boldsymbol{\delta}\mathbf{g}_j^H \mathbf{R}_{\mathbf{p}_j\mathbf{p}_j} \boldsymbol{\delta}\mathbf{g}_j] \\ &+ \text{Re}[\mathbf{g}_j^H \mathbf{R}_{\mathbf{p}_j\mathbf{p}_j^*} \mathbf{g}_j^*] + \text{Re}\{\text{E}_{\boldsymbol{\delta}\mathbf{g}_j}[\boldsymbol{\delta}\mathbf{g}_j^H \mathbf{R}_{\mathbf{p}_j\mathbf{p}_j^*} \boldsymbol{\delta}\mathbf{g}_j^*]\}\Big\} . \end{aligned} \quad (73)$$

The characterization of the perturbation term $\boldsymbol{\delta}\mathbf{g}_j$ is given by the following Lemma.

Lemma 3: Assume that $\mathbf{\Phi}$ is full-column rank and let $\widehat{\mathbf{R}}_{\mathbf{rr}}$ be estimated by (49). Moreover, let $\mathbf{R}_{\mathbf{rr}} = \mathbf{V}_s \mathbf{\Sigma}_s \mathbf{V}_s^H + \sigma_v^2 \mathbf{V}_n \mathbf{V}_n^H$, where $\mathbf{V}_s \in \mathbb{C}^{N\times J}$ collects the eigenvectors associated with the J largest eigenvalues $\mu_1, \mu_2, \ldots, \mu_J$ of $\mathbf{R}_{\mathbf{rr}}$ (arranged in decreasing order), while $\mathbf{V}_n \in \mathbb{C}^{N\times(N-J)}$ collects the eigenvectors associated with the eigenvalue σ_v^2, and, finally, $\mathbf{\Sigma}_s \triangleq \text{diag}(\mu_1, \mu_2, \ldots, \mu_J)$. The *first-order* perturbation term of the L-SMI and L-SUB receivers can be expressed as

$$\boldsymbol{\delta}\mathbf{g}_j = -\mathbf{\Gamma}_{j,\text{L}}\, \widehat{\mathbf{r}}_{\mathbf{p}_j b_j} , \quad (74)$$

where $\widehat{\mathbf{r}}_{\mathbf{p}_j b_j} \triangleq \frac{1}{K}\sum_{k=1}^K \mathbf{p}_j(k)\, b_j(k)$ is the sample cross-correlation between the interference and the desired signal, and

$$\mathbf{\Gamma}_{j,\text{L}} = \begin{cases} \mathbf{P}_{j,\text{L}} \mathbf{R}_{\mathbf{p}_j\mathbf{p}_j}^{-1} , & \text{(L-SMI)} \\ \mathbf{P}_{j,\text{L}} \mathbf{R}_{\mathbf{p}_j\mathbf{p}_j}^{-1} - \gamma_{j,\text{L}} \mathbf{V}_n \mathbf{V}_n^H , & \text{(L-SUB)} \end{cases} \quad (75)$$

with $\mathbf{P}_{j,\text{L}} \triangleq \mathbf{I}_N - (\boldsymbol{\phi}_j^H \mathbf{R}_{\mathbf{p}_j\mathbf{p}_j}^{-1} \boldsymbol{\phi}_j)^{-1} \mathbf{R}_{\mathbf{p}_j\mathbf{p}_j}^{-1} \boldsymbol{\phi}_j \boldsymbol{\phi}_j^H = \mathbf{I}_N - (\boldsymbol{\phi}_j^H \mathbf{R}_{\mathbf{rr}}^{-1} \boldsymbol{\phi}_j)^{-1} \mathbf{R}_{\mathbf{rr}}^{-1} \boldsymbol{\phi}_j \boldsymbol{\phi}_j^H$ and $\gamma_{j,\text{L}} \triangleq \sigma_v^{-2} + (\boldsymbol{\phi}_j^H \mathbf{R}_{\mathbf{rr}}^{-1} \boldsymbol{\phi}_j)^{-1} \boldsymbol{\phi}_j^H \mathbf{V}_s \mathbf{\Omega}_{\text{L}}^{-1} \mathbf{V}_s^H \mathbf{R}_{\mathbf{rr}}^{-1} \boldsymbol{\phi}_j$, where $\mathbf{\Omega}_{\text{L}} \triangleq \mathbf{\Sigma}_{\mathbf{s}} - \sigma_v^2 \mathbf{I}_J \in \mathbb{R}^{J\times J}$.

Proof: The proof is omitted since it is similar to that of Lemma 2. ■

By virtue of Lemma 3, we are now able to evaluate the averages in (73). Specifically, dropping the subscript $\boldsymbol{\delta}\mathbf{g}_j$ in $\text{E}_{\boldsymbol{\delta}\mathbf{g}_j}[\cdot]$ for notational simplicity, we have:

$$\begin{aligned}\text{E}[\boldsymbol{\delta}\mathbf{g}_j^H \mathbf{R}_{\mathbf{p}_j\mathbf{p}_j} \boldsymbol{\delta}\mathbf{g}_j] &= \text{trace}\{\mathbf{\Gamma}_{j,\text{L}}^H \mathbf{R}_{\mathbf{p}_j\mathbf{p}_j} \mathbf{\Gamma}_{j,\text{L}}\, \text{E}[\widehat{\mathbf{r}}_{\mathbf{p}_j b_j} \widehat{\mathbf{r}}_{\mathbf{p}_j b_j}^H]\} \\ &= \frac{1}{K}\, \text{trace}(\mathbf{\Gamma}_{j,\text{L}}^H \mathbf{R}_{\mathbf{p}_j\mathbf{p}_j} \mathbf{\Gamma}_{j,\text{L}} \mathbf{R}_{\mathbf{p}_j\mathbf{p}_j}) , \end{aligned} \quad (76)$$

$$\begin{aligned}\text{E}[\boldsymbol{\delta}\mathbf{g}_j^H \mathbf{R}_{\mathbf{p}_j\mathbf{p}_j^*} \boldsymbol{\delta}\mathbf{g}_j^*] &= \text{trace}\{\mathbf{\Gamma}_{j,\text{L}}^H \mathbf{R}_{\mathbf{p}_j\mathbf{p}_j^*} \mathbf{\Gamma}_{j,\text{L}}^*\, \text{E}[\widehat{\mathbf{r}}_{\mathbf{p}_j b_j}^* \widehat{\mathbf{r}}_{\mathbf{p}_j b_j}^H]\} \\ &= \frac{1}{K}\, \text{trace}(\mathbf{\Gamma}_{j,\text{L}}^H \mathbf{R}_{\mathbf{p}_j\mathbf{p}_j^*} \mathbf{\Gamma}_{j,\text{L}}^* \mathbf{R}_{\mathbf{p}_j\mathbf{p}_j^*}^*) . \end{aligned} \quad (77)$$

By substituting (76) and (77) into (73), and recalling that $\text{SINR}_{j,\text{L-MOE}}{}^{-1} = (\mathbf{g}_j^H \mathbf{R}_{\mathbf{p}_j\mathbf{p}_j} \mathbf{g}_j + \text{Re}[\mathbf{g}_j^H \mathbf{R}_{\mathbf{p}_j\mathbf{p}_j^*} \mathbf{g}_j^*])/2$, we get:

$$\begin{aligned}\text{SINR}(\widehat{\mathbf{g}}_j)^{-1} &= \text{SINR}_{j,\text{L-MOE}}^{-1} \\ &\cdot \Big\{1 + \frac{1}{2K}\Big[\text{trace}(\mathbf{\Gamma}_{j,\text{L}}^H \mathbf{R}_{\mathbf{p}_j\mathbf{p}_j} \mathbf{\Gamma}_{j,\text{L}} \mathbf{R}_{\mathbf{p}_j\mathbf{p}_j}) \\ &+ \text{Re}[\text{trace}(\mathbf{\Gamma}_{j,\text{L}}^H \mathbf{R}_{\mathbf{p}_j\mathbf{p}_j^*} \mathbf{\Gamma}_{j,\text{L}}^* \mathbf{R}_{\mathbf{p}_j\mathbf{p}_j^*}^*)]\Big]\, \text{SINR}_{j,\text{L-MOE}}\Big\} . \end{aligned} \quad (78)$$

Along the same lines of the WL case, it can be shown that

$$\begin{aligned}&\text{trace}(\mathbf{\Gamma}_{j,\text{L}}^H \mathbf{R}_{\mathbf{p}_j\mathbf{p}_j} \mathbf{\Gamma}_{j,\text{L}} \mathbf{R}_{\mathbf{p}_j\mathbf{p}_j}) \\ &= \begin{cases} N-1 , & \text{(L-SMI)} \\ J-1+(N-J)|1-\gamma_{j,\text{L}}\,\sigma_v^2|^2 . & \text{(L-SUB)} \end{cases}\end{aligned} \quad (79)$$

On the other hand, evaluation of the term $\text{trace}(\mathbf{\Gamma}_{j,\text{L}}^H \mathbf{R}_{\mathbf{p}_j\mathbf{p}_j^*} \mathbf{\Gamma}_{j,\text{L}}^* \mathbf{R}_{\mathbf{p}_j\mathbf{p}_j^*}^*)$ is more complicated and, for its calculation, it is convenient to consider the SMI and SUB cases separately. With reference to the L-SMI receiver, since $\mathbf{\Gamma}_{j,\text{L}} = \mathbf{P}_{j,\text{L}} \mathbf{R}_{\mathbf{p}_j\mathbf{p}_j}^{-1}$, after simple algebra, one obtains

$$\begin{aligned}&\text{trace}(\mathbf{\Gamma}_{j,\text{L}}^H \mathbf{R}_{\mathbf{p}_j\mathbf{p}_j^*} \mathbf{\Gamma}_{j,\text{L}}^* \mathbf{R}_{\mathbf{p}_j\mathbf{p}_j^*}^*) \\ &= \text{trace}[\mathbf{R}_{\mathbf{p}_j\mathbf{p}_j}^{-1} \mathbf{P}_{j,\text{L}}^H \mathbf{R}_{\mathbf{p}_j\mathbf{p}_j^*} \mathbf{P}_{j,\text{L}}^* (\mathbf{R}_{\mathbf{p}_j\mathbf{p}_j}^*)^{-1} \mathbf{R}_{\mathbf{p}_j\mathbf{p}_j^*}^*] \\ &= \text{trace}[\mathbf{P}_{j,\text{L}} \mathbf{R}_{\mathbf{p}_j\mathbf{p}_j}^{-1} \mathbf{R}_{\mathbf{p}_j\mathbf{p}_j^*} (\mathbf{P}_{j,\text{L}} \mathbf{R}_{\mathbf{p}_j\mathbf{p}_j}^{-1} \mathbf{R}_{\mathbf{p}_j\mathbf{p}_j^*})^*] \\ &= \text{trace}[\mathbf{P}_{j,\text{L}} \mathbf{R}_{\mathbf{rr}}^{-1} \mathbf{R}_{\mathbf{rr}^*} (\mathbf{P}_{j,\text{L}} \mathbf{R}_{\mathbf{rr}}^{-1} \mathbf{R}_{\mathbf{rr}^*})^*] , \end{aligned} \quad (80)$$

where we used the identities $\mathbf{P}_{j,\text{L}} \mathbf{R}_{\mathbf{p}_j\mathbf{p}_j}^{-1} = \mathbf{R}_{\mathbf{p}_j\mathbf{p}_j}^{-1} \mathbf{P}_{j,\text{L}}^H$ and $\mathbf{P}_{j,\text{L}} \mathbf{R}_{\mathbf{p}_j\mathbf{p}_j}^{-1} \mathbf{R}_{\mathbf{p}_j\mathbf{p}_j^*} = \mathbf{P}_{j,\text{L}} \mathbf{R}_{\mathbf{rr}}^{-1} \mathbf{R}_{\mathbf{rr}^*}$. To obtain a more manageable expression of $\text{trace}(\mathbf{\Gamma}_{j,\text{L}}^H \mathbf{R}_{\mathbf{p}_j\mathbf{p}_j^*} \mathbf{\Gamma}_{j,\text{L}}^* \mathbf{R}_{\mathbf{p}_j\mathbf{p}_j^*}^*)$, we consider its asymptotic value as $\sigma_v^2 \to 0$, i.e., in the high-SNR regime. By accounting for the expression of $\mathbf{P}_{j,\mathrm{L}}$ given by Lemma 3, observing that, under assumptions **(a1)** and **(a2)**, $\mathbf{R}_{\mathbf{rr}} = \mathbf{\Phi}\,\mathbf{\Phi}^H + \sigma_v^2\,\mathbf{I}_N$ and $\mathbf{R}_{\mathbf{rr}^*} = \mathbf{\Phi}\,\mathbf{\Phi}^T$, and resorting to the limit formula for the Moore-Penrose inverse [19], one has

$$\begin{aligned}
&\lim_{\sigma_v^2 \to 0} \mathbf{P}_{j,\mathrm{L}}\,\mathbf{R}_{\mathbf{rr}}^{-1}\,\mathbf{R}_{\mathbf{rr}^*} \\
&\quad = \lim_{\sigma_v^2 \to 0} \left\{ \left[\mathbf{I}_N - \frac{(\mathbf{\Phi}\,\mathbf{\Phi}^H + \sigma_v^2 \mathbf{I}_N)^{-1}\mathbf{\Phi}\,\mathbf{1}_j\,\boldsymbol{\phi}_j^H}{\boldsymbol{\phi}_j^H(\mathbf{\Phi}\mathbf{\Phi}^H + \sigma_v^2\mathbf{I})^{-1}\mathbf{\Phi}\,\mathbf{1}_j} \right] \right. \\
&\qquad \left. \cdot (\mathbf{\Phi}\,\mathbf{\Phi}^H + \sigma_v^2\,\mathbf{I}_N)^{-1}\mathbf{\Phi}\,\mathbf{\Phi}^T \right\} \\
&\quad = \left[\mathbf{I}_N - \frac{(\mathbf{\Phi}^H)^\dagger \mathbf{1}_j\,\boldsymbol{\phi}_j^H}{\boldsymbol{\phi}_j^H(\mathbf{\Phi}^H)^\dagger\,\mathbf{1}_j} \right] (\mathbf{\Phi}^H)^\dagger \mathbf{\Phi}^T \\
&= \left[\mathbf{I}_N - (\mathbf{\Phi}^H)^\dagger \mathbf{1}_j\,\mathbf{1}_j^T \mathbf{\Phi}^H \right] (\mathbf{\Phi}^H)^\dagger \mathbf{\Phi}^T = (\mathbf{\Phi}^H)^\dagger\,\mathbf{S}_j\,\mathbf{\Phi}^T
\end{aligned} \tag{81}$$

where $\mathbf{1}_j \triangleq [\overbrace{0,\ldots,0}^{j-1},1,0,\ldots,0]^T \in \mathbb{R}^{J\times 1}$ and $\mathbf{S}_j \triangleq \mathbf{I}_J - \mathbf{1}_j\,\mathbf{1}_j^T \in \mathbb{R}^{J\times J}$. Accounting for (81), the asymptotic value of (80) is given by

$$\begin{aligned}
&\lim_{\sigma_v^2 \to 0} \mathrm{trace}(\mathbf{\Gamma}_{j,\mathrm{L}}^H\,\mathbf{R}_{\mathbf{p}_j\mathbf{p}_j^*}\,\mathbf{\Gamma}_{j,\mathrm{L}}^*\,\mathbf{R}_{\mathbf{p}_j\mathbf{p}_j^*}^*) \\
&\qquad = \mathrm{trace}\left[\mathbf{S}_j\,\mathbf{\Phi}^T(\mathbf{\Phi}^T)^\dagger\,\mathbf{S}_j\right] \\
&\qquad = \mathrm{trace}\left[\mathbf{\Phi}^T(\mathbf{\Phi}^T)^\dagger\,\mathbf{S}_j\right] = J-1\,.
\end{aligned} \tag{82}$$

As regards the L-SUB receiver, since $\mathbf{\Gamma}_{j,\mathrm{L}} = \mathbf{P}_{j,\mathrm{L}}\,\mathbf{R}_{\mathbf{p}_j\mathbf{p}_j}^{-1} - \gamma_{j,\mathrm{L}}\,\mathbf{V}_n\,\mathbf{V}_n^H$, recalling that $\mathbf{R}_{\mathbf{p}_j\mathbf{p}_j^*} = \overline{\mathbf{\Phi}}_j\,\overline{\mathbf{\Phi}}_j^T$, and observing that $\mathbf{V}_n^H\,\overline{\mathbf{\Phi}}_j = \mathbf{O}_{(N-J)\times(J-1)}$, it follows that $\mathrm{trace}(\mathbf{\Gamma}_{j,\mathrm{L}}^H\,\mathbf{R}_{\mathbf{p}_j\mathbf{p}_j^*}\,\mathbf{\Gamma}_{j,\mathrm{L}}^*\,\mathbf{R}_{\mathbf{p}_j\mathbf{p}_j^*}^*) = \mathrm{trace}[\mathbf{R}_{\mathbf{p}_j\mathbf{p}_j}^{-1}\,\mathbf{P}_{j,\mathrm{L}}^H\,\overline{\mathbf{\Phi}}_j\,\overline{\mathbf{\Phi}}_j^T\,\mathbf{P}_{j,\mathrm{L}}^*\,(\mathbf{R}_{\mathbf{p}_j\mathbf{p}_j}^*)^{-1}\,\overline{\mathbf{\Phi}}_j^*\,\overline{\mathbf{\Phi}}_j^H] = \mathrm{trace}[\mathbf{R}_{\mathbf{p}_j\mathbf{p}_j}^{-1}\,\mathbf{P}_{j,\mathrm{L}}^H\mathbf{R}_{\mathbf{p}_j\mathbf{p}_j^*}\,\mathbf{P}_{j,\mathrm{L}}^*\,(\mathbf{R}_{\mathbf{p}_j\mathbf{p}_j}^*)^{-1}\mathbf{R}_{\mathbf{p}_j\mathbf{p}_j^*}^*]$, which turns out to be exactly equal to (80). Thus, in conclusion, by substituting (79) and (82) into (78), eqs. (51) and (52) are obtained by additionally observing that, with reference to the L-SUB receiver, $\gamma_{j,\mathrm{L}}\,\sigma_v^2 \to 1$ as $\sigma_v^2 \to 0$.

REFERENCES

[1] S. Verdú, "Minimum probability of error for asynchronous Gaussian multiple-access channels," *IEEE Trans. Inform. Theory*, vol. 32, no. 1, pp. 85–96, Jan. 1986.

[2] R. Lupas and S. Verdú, "Linear multiuser detectors for synchronous code-division multiple access channels," *IEEE Trans. Inform. Theory*, vol. 35, no. 1, pp. 123–136, Jan. 1989.

[3] U. Madhow and M. Honig, "MMSE interference suppression for direct-sequence spread-spectrum CDMA," *IEEE Trans. Commun.*, vol. 42, no. 12, pp. 3178–3188, Dec. 1994.

[4] M. Honig, U. Madhow, and S. Verdú, "Blind adaptive multiuser detection," *IEEE Trans. Inform. Theory*, vol. 41, no. 4, pp. 944–960, July 1995.

[5] F.D. Neeser and J.L. Massey, "Proper complex random processes with applications to information theory," *IEEE Trans. Inform. Theory*, vol. 39, no. 4, pp. 1293–1302, July 1993.

[6] B. Picinbono and P. Chevalier, "Widely linear estimation with complex data," *IEEE Trans. Signal Processing*, vol. 43, no. 8, pp. 2030–2033, Aug. 1995.

[7] G. Gelli, L. Paura, and A. R. P. Ragozini, "Blind widely linear multiuser detection," *IEEE Commun. Lett.*, vol. 4, no. 6, pp. 187–189, June 2000.

[8] S. Buzzi, M. Lops, and A.M. Tulino, "A new family of MMSE multiuser receivers for interference suppression in DS-CDMA systems employing BPSK modulation," *IEEE Trans. Commun.*, vol. 49, no. 1, pp. 154–167, Jan. 2001.

[9] R. Schober, W.H. Gerstacker, and L. Lampe, "On suboptimum receivers for DS-CDMA with BPSK modulation," *Signal Processing*, vol. 85, no. 7, pp. 1149–1163, 2005.

[10] J-J. Jeon, J. G. Andrews, and K.-M. Sung, "The blind widely linear minimum output energy algorithm for DS-CDMA systems", *IEEE Trans. Signal Processing*, vol. 54, no. 5, pp. 1926–1931, May 2006.

[11] S. Buzzi, M. Lops, and A.M. Tulino, "A generalized minimum-mean-output-energy strategy for CDMA systems with improper MAI," *IEEE Trans. Inform. Theory*, vol. 48, no. 3, pp. 761–767, Mar. 2002.

[12] A. M. Tulino and S. Verdú, "Asymptotic analysis of improved linear receivers for BPSK-CDMA subject to fading," *IEEE J. Select. Areas Commun.*, vol. 19, no. 8, pp. 1544–1555, Aug. 2001.

[13] Y. Yoon and K.-M. Kim, "An efficient blind multiuser detection for improper DS/CDMA signals", *IEEE Trans. Veh. Technol.*, vol. 55, no. 2, pp. 572–582, Mar. 2006.

[14] A. Lampe and M. Breiling, "Asymptotic analysis of widely linear MMSE multiuser detection – complex vs real modulation," in *Proc. of the Information Theory Workshop (ITW) 2001*, Cairns, Australia, September 2001, pp. 55–57.

[15] D. N. C. Tse and S. V. Hanly, "Linear multiuser receivers: effective interference, effective bandwidth and user capacity," *IEEE Trans. Inform. Theory*, vol. 45, no. 2, pp. 641–657, Mar. 1999.

[16] S. Buzzi and M. Lops, "Performance analysis for the improved linear multiuser detectors in BPSK-modulated DS-CDMA systems," *IEEE Trans. Commun.*, vol. 51, no. 1, pp. 37–42, Jan. 2003.

[17] P.J. Schreier, L.L. Scharf, and C.T. Mullis, "Detection and estimation of improper complex random signals," *IEEE Trans. Inform. Theory*, vol. 51, no. 1, pp. 306–312, Jan. 2005.

[18] R. Schober, W. H. Gerstacker, and L.H.-J. Lampe, "Data-aided and blind stochastic gradient algorithms for widely linear MMSE MAI suppression for DS-CDMA", *IEEE Trans. Signal Processing*, vol. 52, no. 3, pp. 746–756, Mar. 2004.

[19] A. Ben-Israel and T. N. E. Greville, *Generalized Inverses*, New York: Springer-Verlag, 2002.

[20] S. V. Schell, "A separability theorem for $2M$ conjugate-symmetric signals impinging on an M-element sensor array," *IEEE Trans. Signal Processing*, vol. 45, no. 3, pp. 789–792, Mar. 1997.

[21] D. Darsena, G. Gelli, L. Paura, and F. Verde, "Subspace-based blind channel identification of SISO-FIR systems with improper random inputs," *Signal Processing, Special Issue on Signal Processing in Communications*, vol. 84, no. 11, pp. 2021–2039, Nov. 2004.

[22] D. Darsena, G. Gelli, L. Paura, and F. Verde, "Widely-linear equalization and blind channel identification for interference-contaminated multicarrier systems", *IEEE Trans. Signal Processing*, vol. 53, no. 3, pp. 1163–1177, Mar. 2005.

[23] G. Gelli and F. Verde, "Blind subspace-based channel identification for quasi-synchronous MC-CDMA systems employing improper data symbols," in *Proc. of the 14th European Signal Processing Conference (EUSIPCO)*, Florence, Italy, Sep. 2006.

[24] D. Mattera, L. Paura, and F. Sterle, "Widely linear decision-feedback equalizer for time-dispersive linear MIMO channels," *IEEE Trans. Signal Processing*, vol. 53, no. 7, pp. 2525–2536, July 2005.

[25] M.K. Varanasi, "Group detection for synchronous Gaussian code-division multiple-access channels," *IEEE Trans. Inform. Theory*, vol. 41, no. 4, pp. 1083–1096, July 1995.

[26] A. Kapur and M. K. Varanasi, "Multiuser detection for overloaded CDMA systems," *IEEE Trans. Inform. Theory*, vol. 49, no. 7, pp. 1728–1742, July 2003.

[27] P.J. Schreier and L.L. Scharf, "Second-order analysis of improper complex random vectors and processes," *IEEE Trans. Signal Processing*, vol. 51, no. 3, pp. 714–725, Mar. 2003.

[28] M. Honig and M. K. Tsatsanis, "Adaptive techniques for multiuser CDMA receivers", *IEEE Signal Processing Magazine*, vol. 17, no. 3, pp. 49–61, May 2000.

[29] R. A. Horn and C. R. Johnson, *Matrix Analysis*, Cambridge: Cambridge University Press, 1990.

[30] H.V. Poor and S. Verdù, "Probability of error in MMSE multiuser detection," *IEEE Trans. Inform. Theory*, vol. 43, no. 5, pp. 868–871, May 1997.

[31] F. Li, H. Liu, and R.J. Vaccaro "Performance analysis for DOA estimation algorithms: unification, simplification, and observations," *IEEE Trans. Aerospace and Electronic Systems*, vol. 29, no. 4, pp. 1170–1184, Oct. 1993.

[32] Z. Xu and X. Wang, "Large-sample performance of blind and group-blind multiuser detectors: A perturbation perspective," *IEEE Trans. Inform. Theory*, vol. 50, no. 10, pp. 2389–2401, Oct. 2004.
[33] M. Wax and Y. Anu, "Performance analysis of the minimum variance beamformer," *IEEE Trans. Signal Processing*, vol. 44, no. 4, pp. 928–937, Apr. 1996.
[34] M.K. Tsatsanis and Z.D. Xu, "Performance analysis of minimum variance CDMA receivers," *IEEE Trans. Signal Processing*, vol. 46, no. 11, pp. 3014–3022, Nov. 1998.

Angela Sara Cacciapuoti was born in Pozzuoli, Italy, on August 19, 1980. She received the Dr. Eng. degree *summa cum laude* in telecommunications engineering in 2005 from the University of Napoli Federico II. She is currently a Ph.D. student in electronic and telecommunications engineering at the Department of Electronic and Telecommunication Engineering, University of Napoli Federico II.

Her research activities lie in the area of statistical signal processing, digital communications, and communication systems. In particular, her current interests are focused on equalization, channel identification, and multiuser detection.

Giacinto Gelli was born in Napoli, Italy, on July 29, 1964. He received the Dr. Eng. degree *summa cum laude* in electronic engineering in 1990, and the Ph.D. degree in computer science and electronic engineering in 1994, both from the University of Napoli Federico II, Italy.

From 1994 to 1998, he was an Assistant Professor with the Department of Information Engineering, Second University of Napoli. Since 1998 he has been with the Department of Electronic and Telecommunication Engineering, University of Napoli Federico II, first as an Associate Professor, and since November 2006 as a Full Professor of Telecommunications. He also held teaching positions at the University Parthenope of Napoli. His research interests are in the fields of statistical signal processing, array processing, image processing, and mobile communications, with current emphasis on code-division multiple-access systems and multicarrier modulation.

Luigi Paura was born in Napoli, Italy, on February 20, 1950. He received the Dr. Eng. degree *summa cum laude* in electronic engineering in 1974 from the University of Napoli Federico II.

From 1979 to 1984 he was with the Department of Electronic and Telecommunication Engineering, University of Napoli, Italy, first as an Assistant Professor and then as an Associate Professor. Since 1994, he has been a Full Professor of Telecommunications: first, with the Department of Mathematics, University of Lecce, Italy; then, with the Department of Information Engineering, Second University of Napoli; and, finally, from 1998 he has been with the Department of Electronic and Telecommunication Engineering, University of Napoli Federico II. He also held teaching positions at the University of Salerno, Italy, at the University of Sannio, Italy, and the University Parthenope, Napoli, Italy. In 1985-86 and 1991 he was a Visiting Researcher at the Signal and Image Processing Laboratory, University of California, Davis. At the present time, his research activities are mainly concerned with statistical signal processing, digital communication systems and medium access control in wireless networks.

Francesco Verde was born in Santa Maria Capua Vetere, Italy, on June 12, 1974. He received the Dr. Eng. degree *summa cum laude* in electronic engineering in 1998 from the Second University of Napoli, and the Ph.D. degree in information engineering in 2002, from the University of Napoli Federico II.

Since 2002, he has been an Assistant Professor of Signal Theory with the Department of Electronic and Telecommunication Engineering, University of Napoli Federico II. He also held teaching positions at the Second University of Napoli. His research activities lie in the area of statistical signal processing, digital communications, and communication systems. In particular, his current interests are focused on cyclostationarity-based techniques for blind identification, equalization and interference suppression for narrowband modulation systems, code-division multiple-access systems, and multicarrier modulation systems.